8971-0003-RU-000

REPRODUCIBILITY STUDIES ON CIRCUITS EMPLOYING THIN FILM SUPERCONDUCTORS FORMED BY VACUUM DEPOSITION

by

A. J. Learn and R. S. Spriggs

10 October 1961

This work was supported in part by the Independent Research Program of Space Technology Laboratories, Inc. and in part by the Office of Naval Research, Contract Nonr 2542(00).

RESEARCH LABORATORY
Space Technology Laboratories, Inc.
P. O. Box 95001
Los Angeles 45, California

ABSTRACT

Thin-film cryotrons with tin gate thickness reproducible to within 5% and lead control films having less than one micron penumbra have been fabricated. For such films, formed under carefully controlled evaporation conditions, tin critical temperatures are reproducible to within $0.005^{\circ}K$ and critical currents for the cryotron to about $\pm 5\%$ with comparable tolerances for the low temperature resistivity of the tin. A detailed discussion of apparatus designed for control of evaporation parameters and film geometry is given. Study of film formation through monitoring of film conductance has yielded information regarding the nature of the scattering of conduction electrons at the walls of the film. Films formed at or annealed at room temperature show purely spectral scattering. In addition, such studies reveal a minimum critical thickness for onset of electrical conduction of about 90 Å for both tin and lead. This value is obtained for very large deposition rates independent of substrate temperature.

CONTENTS

FIGURES

FIGURES (Continued)

I. INTRODUCTION

Formation of a single evaporated film relatively free from impurities, with sharp edges, and of a desired thickness so that its superconducting properties are reproducible is a problem which has been dealt with in great detail.[1, 2, 3] Building up successive layers of such films to form a reproducible circuit represents an order of magnitude increase in difficulty. To ensure resistanceless contact between layers of metal it is imperative that the vacuum not be broken between depositions. This is also important in limiting the opportunities for contamination of metal layers which are subsequently to be covered by an insulating film. Provision must be made then for evaporation of several materials and interposition of several differently shaped masks between source and substrate during a single evacuation. A desire to test the reproducibility of at least two circuits made during a single evacuation compounds the problems somewhat.

The particular multilayer structure concentrated on was the thin-film cryotron composed of a lead ground shield, tin gate, and lead control with layers of polymer insulation between metal films. Cryotron operation entails switching of the gate film from the superconducting state to the resistive state by the combination of current flowing directly through the gate and the magnetic field generated by a current in the control film The control ideally remains in the superconducting state regardless of the magnitude of the current it carries. The edge region normally associated with evaporated films, where the thickness is less than that of the main body of the film, can lead to unwanted switching of the control film or unpredictable switching behavior for the gate film. Thus it is important not only to exercise control of film thickness in the main body of the film but also to minimize the extent of the film edge so that the resulting film has uniform thickness across its entire width

For single films, lands of material (e g., indium solder) serve to provide contact to the evaporated film and also contact to an external circuit where the resistance (and hence thickness) of the film can be

observed. The mask can be placed in physical contact with the substrate, thus ensuring small penumbra for films somewhat independent of source dimensions and source-substrate distance. Thus a simple planar strip vapor source may be used and high deposition rates result with little heating. A minimum amount of shielding and cooling then ensures low pressures during deposition and acceptably small impurity content.

In multilayer circuits, limiting the penumbra becomes more of a problem. Masks cannot be placed directly against the substrate since this would result in destruction of films previously deposited. Thus the source dimensions, source-mask distance, and mask-substrate distance are highly relevant. Sources must be found which are not only of small dimension, but which deliver reasonable and uniform deposition rates while deposition pressures remain acceptably low. Deposition rates, of course, also depend on source-substrate distance and here again a compromise must be made. Further, means must be provided for adjusting mask-substrate distances.

Another step involves making electrical contact to the film during deposition so that its conductance can be monitored. Finally, sufficiently sensitive and automatic recording equipment must be designed and assembled.

Methods and equipment have been developed which are generally applicable to formation of thin-film circuitry by evaporation and these are described in the following pages. The conditions under which geometrically reproducible cryotrons could be produced were determined and a study made of the resultant uniformity of their electrical and superconducing properties.

II. APPARATUS AND PROCEDURE

The assembled vacuum system employed in this study is shown in Fig. 1. The labelled components within the volume defined by the bell jar and the top and base plates will be described and their functions discussed in Sections II. A-E. This volume is evacuated by a Consolidated Electrodynamic Corp., Type MCF 300, 4-inch diffusion pump employing DOW Corning 704 silicone oil. A CEC water-cooled Baffle, Type WB-40, is positioned between the diffusion pump and base plate. This baffle is maintained at 278°K with a recirculating refrigeration unit.

A. Vapor Sources and Pressure Control

The vapor sources presently in use are radiatively heated isothermal ovens with a small tubular opening as shown in Fig. 2. These consist of a molybdenum container, with a press fit top, fitted into four thin tantalum sheets through which current is passed. The tantalum sheets are anchored at either end by heavier copper bars. Once the oven reaches an equilibrium temperature, the deposition rate remains quite uniform nearly until the evaporation of the last remnant of material in the oven. The current-voltage setting for the vapor sources did not prove to be a good measure of source temperature and hence deposition rate. Consequently, if a particular deposition rate was desired, one specimen was monitored during the warmup period for the source and the source temperature adjusted until the desired rate of change of conductance was obtained. Then evaporations were performed on the remaining substrates. With the substrate located 8.5" from the source, typical deposition rates were 25 Å/sec for tin and 50 Å/sec for lead.

The uniformity of the spatial flux distribution of such pseudo-point sources was found to depend markedly on the ratio of the length of the cylindrical opening to its diameter, being much more sharply concentrated directly above the source for a long narrow opening. By suitably shortening the opening, areas about 3" in diameter located 10" from the source could be coated with less than 5% variation in thickness.

Figure 1 - Vapor Deposition Unit Used for Producing Cryotrons. Lettered Components Are Discussed in Detail in Text.

A - Radiation Shield
B - Liquid Nitrogen-Cooled Surfaces
C - Collimating Slits
D - Electron Gun
E - Oil Source
F - Crosshairs
G - Pointer
H - Mirror
I - Mask Support Wheel
J - Masks
K - Substrate Well
L - Vernier
M - Ionization Gauge
N - Electrical Leads to Probes

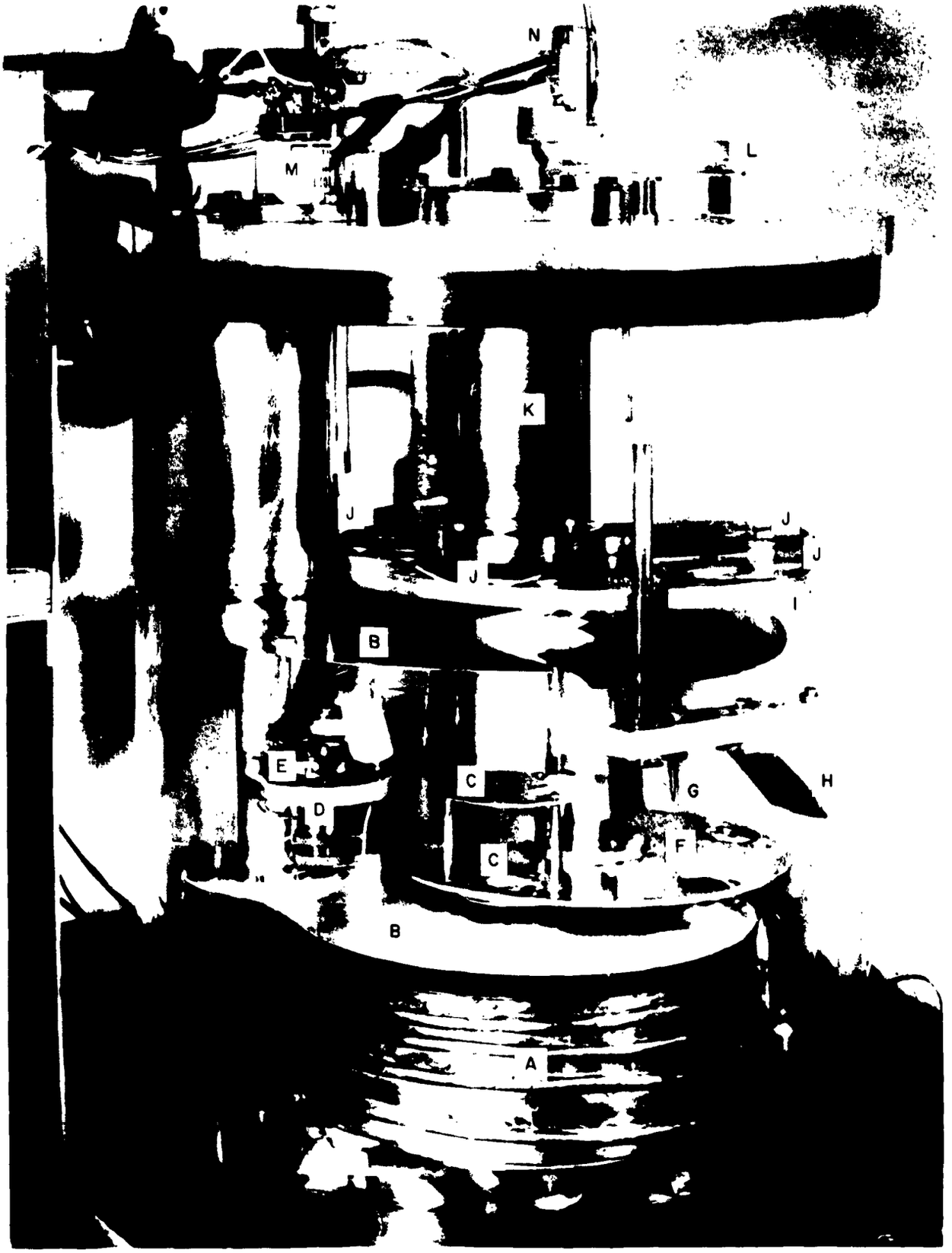

Figure 1

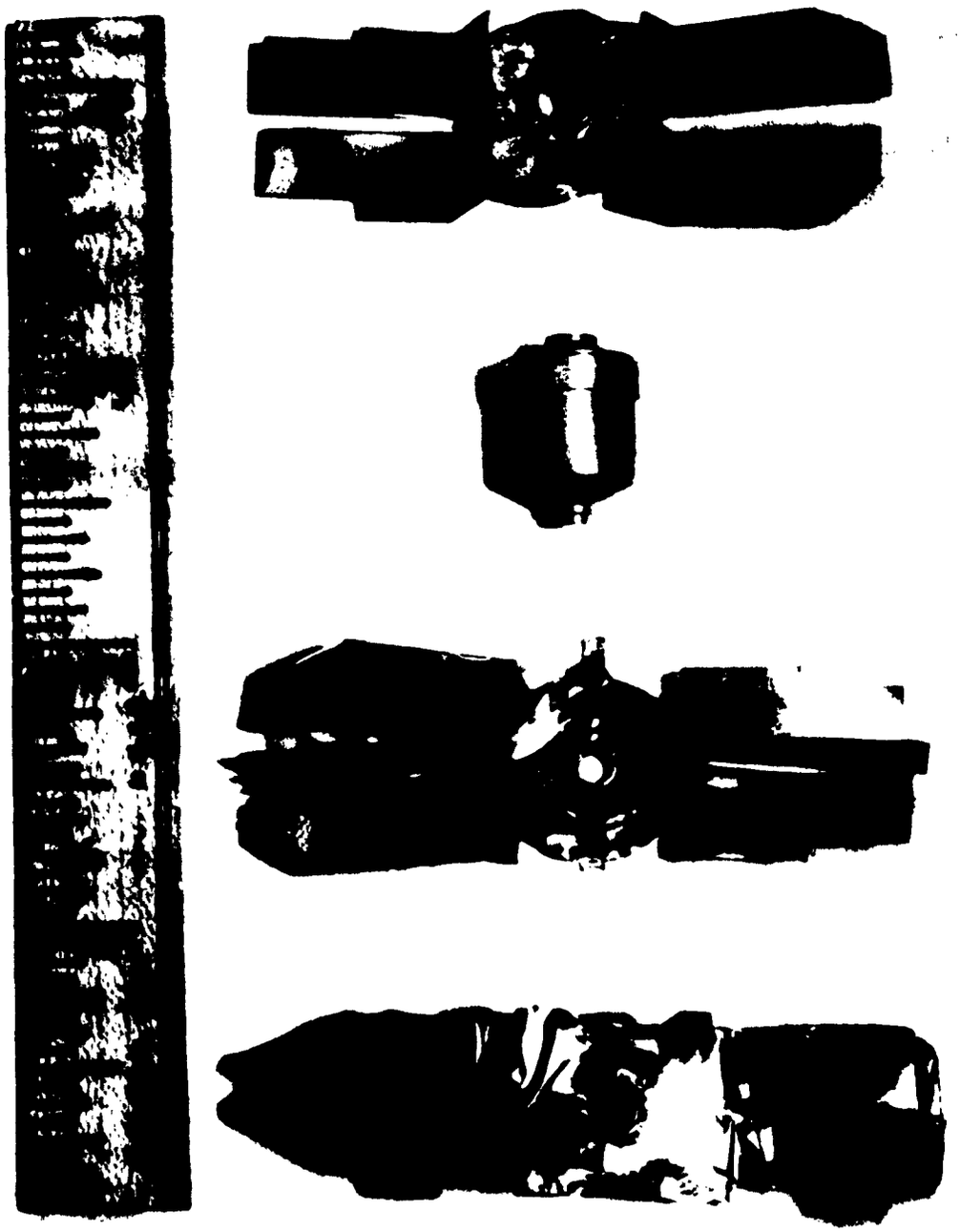

Figure 2 - Vapor Source. Upper Portion Shows Molybdenum Container and Heater Strips Separately.

One end of all sources for a given fabrication is attached to a common shaft rotatable from outside the vacuum system as shown in Fig. 3. This shaft lies near the center of the radiation shield which surrounds the vapor-source assembly. The shield acts as a limiting stop so that radiation is received only from the molten metal and not the heater strips. Inside near the circumference of the shield lies a second vertical shaft which extends outside the vacuum system and provides contact to the other end of the particular source selected for an evaporation. This consists of a fixed outer cylinder and lip and a central hat of adjustable elevation which clamps the selected source in position. The electrodes are hollow so that water may be circulated through them during heating of the vapor sources as well as through the coils wound about the shielding tower. The electrodes are in a chamber separated from the remainder of the tower by walls forming a sector. This prevents contamination of other vapor sources during heating of a particular one. Also this chamber may be out-gassed by heating up an auxiliary strip before deposition begins. The body of the tower is out-gassed by passing live steam through the coils about it during the initial pumping of the vacuum system. The steam is also circulated through the hollow source electrodes. A Mylar sheet is placed around the bell jar and hot air circulated through the space between them to aid in out-gassing the bell jar and top plate. Once the system has been out-gassed, cold water is passed through the coils about the shielding tower and through the source electrodes. In addition there are two large surfaces cooled to liquid nitrogen temperature which act as pumps for vapors condensible at that temperature; e.g., carbon dioxide and water vapor. After these heating and cooling steps, pressure during deposition can be maintained at less than 5×10^{-7} mm Hg. with the deposition rates quoted above. The ionization pressure gauge was mounted directly in the top plate, as far from the diffusion pump as possible, so its reading should represent an upper value for the system pressure.

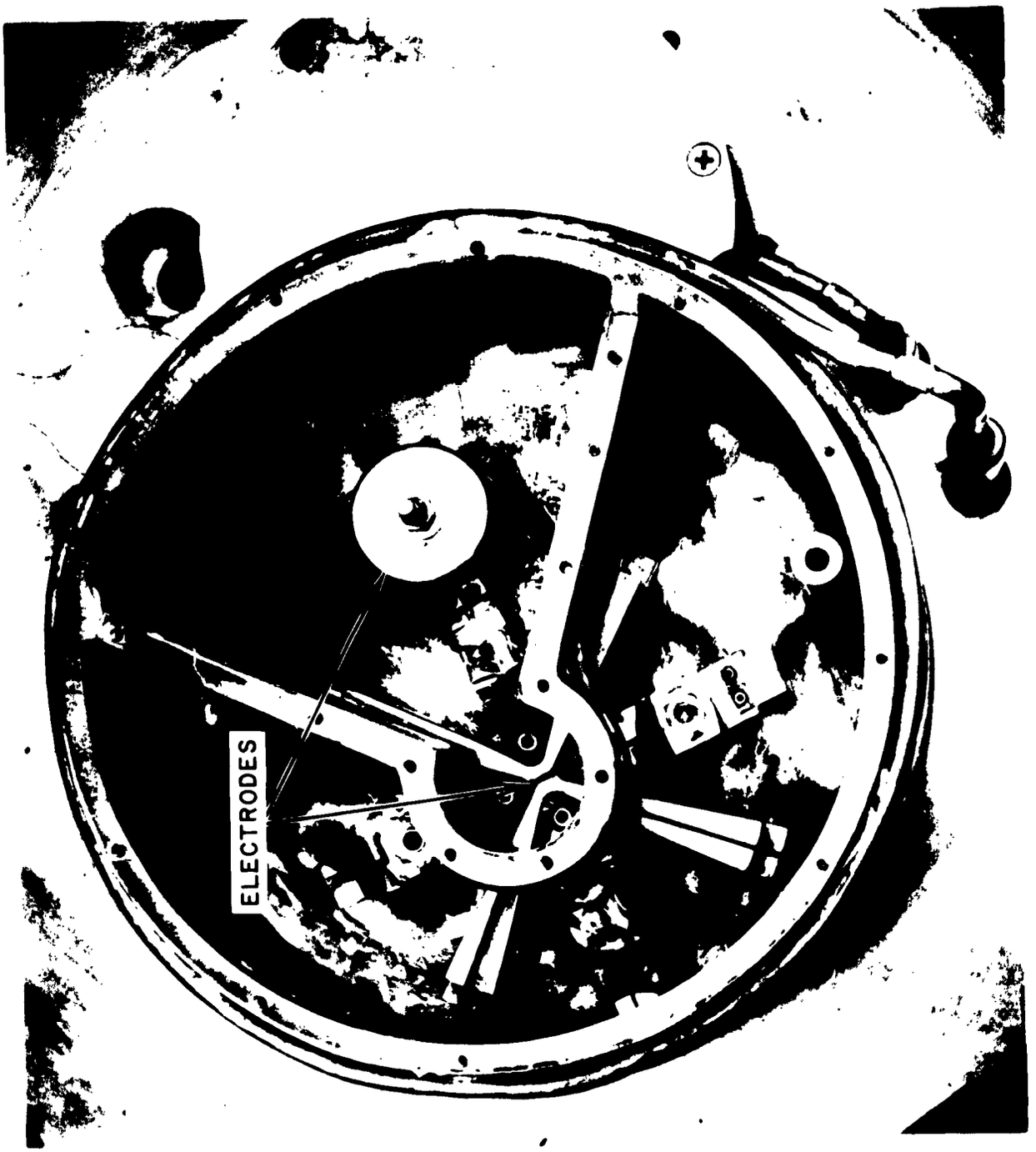

Figure 3 - Vapor Sources Mounted on Rotatable Electrode Within Radiation Shield

Conservative estimates of concentrations of gases which may be present during deposition of a tin film on a substrate at room temperature, without deterimental effects on the characteristics of the transition from the superconducting state to the normal state induced by an external magnetic field, have been established.[4] For a deposition rate of 50 Å/sec, the allowable partial pressure P in millimeters of mercury for various gases likely to be present in the vacuum system are:

$$P_{(O_2)} < 5 \times 10^{-8}$$

$$P_{(H_2O)} < 4 \times 10^{-7}$$

$$P_{(CO_2)} < 8 \times 10^{-7}$$

$$P_{(N_2,\ CO,\ CH_4)} < 10^{-5}$$

The presence of impurities in the thinner regions of the film near the edge was manifested at about these partial pressures but the properties of the bulk of the film were not affected appreciably until the partial pressures became an order of magnitude larger. Thus if special care is taken to obtain sharp film edges then allowable partial pressures may be an order of magnitude larger than those listed above.

Edges on our tin films were quite sharp due to the heating which they experienced during parts of the fabrication procedure (c.f. Sec. II. D). This led to agglomeration of the thinner portions of the film and their resultant separation from the main body of the film. Thus, disregarding the differences which evaporation on a cooled substrate may make in the allowable partial pressures, total deposition pressures of less than 5×10^{-7} mm Hg for a tin deposition rate of about 25 Å/sec seem to be within a safe range. This is particularly true if only a small portion of this pressure is accounted for by oxygen molecules. The problem of impurities in the lead film is perhaps less severe since all that is required in this case is to prevent transition of any of its regions to the normal state. This can be done by limiting the extent of its edges and thus eliminating thin regions of the film.

B. Substrate Preparation

Films are deposited on quartz or glass discs 1" in diameter and 1/8" thick. Either material may be mechanically polished to give a surface free from scratches and optically flat. A careful cleaning procedure is carried out involving a hand wash in detergent, ultrasonic rinse in distilled water, immersion in boiling distilled water, and finally a vapor degreasing. The cleanliness of the substrate at any point in the procedure may be tested by observing the uniformity with which a drop of distilled water spreads over its surface. Clean substrates are mounted on the stainless steel well of Fig. 1, the temperature of which may be controlled externally by addition of coolants or insertion of a heater. To ensure good thermal contact between substrate and well, a smear of vacuum grease is placed under the substrate before it is glued on with Duco cement. A copper-constantan or chromel-alumel thermocouple is attached to the well near the substrate. Attachment of a second thermocouple directly to the substrate established that the correlation between well temperature and substrate temperature was sufficiently good so that the former temperature gave an adequate indication of substrate temperature.

Substrates are sufficiently far removed from the sources and thermal contact to the well is good enough so that the substrate temperature does not measurably increase due to radiation from the source during the course of evaporations lasting a few minutes.

C. Masks and Collimator

The masks used to shape the desired circuits are mounted on a wheel which may be rotated from outside the system, thus bringing any one of five masks into position beneath the substrate. The wheel is also mounted on an adjustable screw mechanism so that its elevation can be changed. A locking mechanism guarantees accurate registration of different masks once they have been individually centered and aligned on the wheel. Each mask consists of four sub-masks as shown in Fig. 4 which allows four geometrically similar circuits to

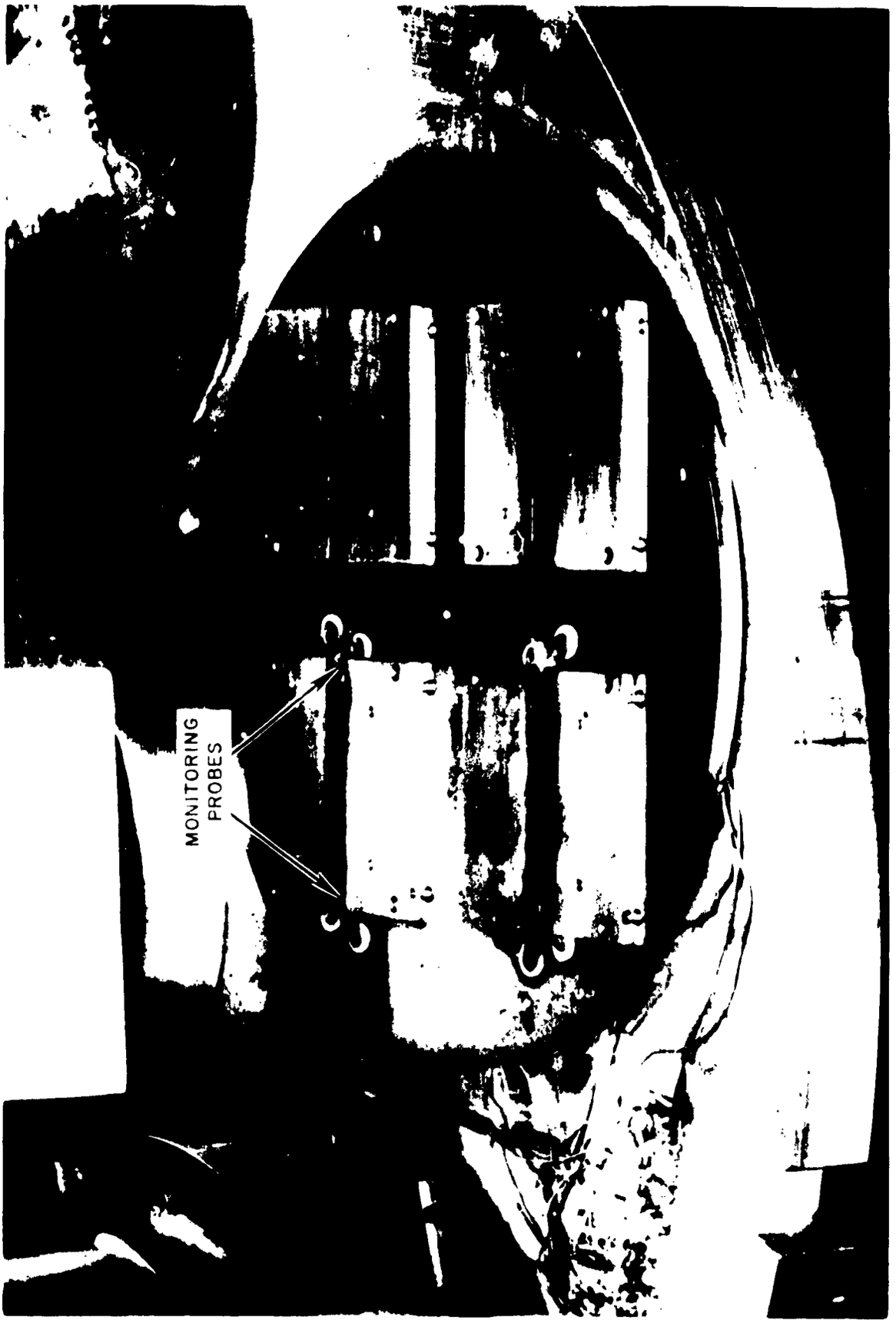

Figure 4 - Individual Group of Four Masks Mounted on Rotatable Wheel

be built up on four different substrates during a single evacuation. The knife edges comprising the mask are ground and mounted at an angle to the incident atomic flux such that the probability of atoms being scattered from the front surface of one blade behind the other blade is minimized. The mounting for the blades ensures that they are coplanar to within 0.001".

Mounted on but insulated from the mask are a pair of copper-beryllium probes at each end of the masking slit. If contact material (lead) has previously been evaporated into the electrode areas, continuity between pairs serves to signal a selected distance of approach between mask and substrate. The extent of the probes above the mask can be adjusted to approximately 0.001". With this mask substrate separation d, a source mask distance R = 8.5", and a lead vapor source opening s = 3/32", a penumbra of several microns was observed although when calculated from the relationship $d(^{s}/R)$ it should be less than 1/2μ. For lead deposition rates of about 50 Å/sec, the density of lead atoms near the source is sufficiently high that frequent collisions occur, thus giving rise to a source effectively much larger than the actual source. Installation of a set of collimating slits above the lead source ensures that only those atoms rising directly from the chimney of the oven reach the substrate. Accurate alignment of the vapor source is then necessary so that the entire source is visible through the masking slit and collimator at the substrate; if this is not true, a film of varying thickness across its width results. A combination of vernier, pointer, crosshairs, and mirror enable alignment of vapor source and top plate to within 0.06".

D. Deposition of Insulating Films

Layers of insulation, which must be present between layers of superconducting metal, are formed by polymerization of silicone oil bombarded by electrons.[5] The electron spray required is provided by an electron gun mounted on a rotatable arm so that it may be brought into position beneath the substrates. In addition, the gun is provided

with a nearly circular motion such that it travels at about 5 rpm beneath the centers of each of the four substrates during deposition. The oil is supplied at any desired rate by heating a copper ring source container warmed by nichrome heater wires. A thermocouple is attached to the oil source and the rate of oil deposition controlled by the source temperature. Typical insulation deposition rates are 25 Å/min. After formation of the insulation, the substrate is heated to drive off any undecomposed oil in readiness for the next metal evaporation. It was found that, for insulation deposited on a lead ground shield, exceeding a temperature of about 340°K resulted in sufficient expansion of the insulating film to cause its rupture. After cooling to deposition temperature for the metal, new material is evaporated in the electrode areas to guarantee good contact by the probes when the masks are again brought in near proximity to the substrates. In such heating and cooling processes about five minutes must be allowed for the front surface of the quartz substrate to reach the well temperature. Somewhat longer times were required to reach thermal equilibrium when glass was used as substrate material.

Some difficulty was experienced at times in obtaining and retaining electrical insulation due to large particles ejected during the lead ground plane or tin gate evaporation. If a particle appeared in the lead film it could not be adequately covered. Particles released in the tin evaporation would punch a hole in the existing insulation upon impact with the substrate. The particles could either be formed of atoms like the material being evaporated or of foreign atoms. For very large evaporation rates, lumps of the material being evaporated were forced out of the opening to the oven source. After use of a source for many evaporations, during which some amount of alloying had taken place at the oven walls, particles composed of foreign atoms could appear.

E. Film Conductance Monitoring

The spacing probes mentioned above provide a means for monitoring the film conductance during deposition and hence film thickness. Electrical leads to the probes are brought out of the system

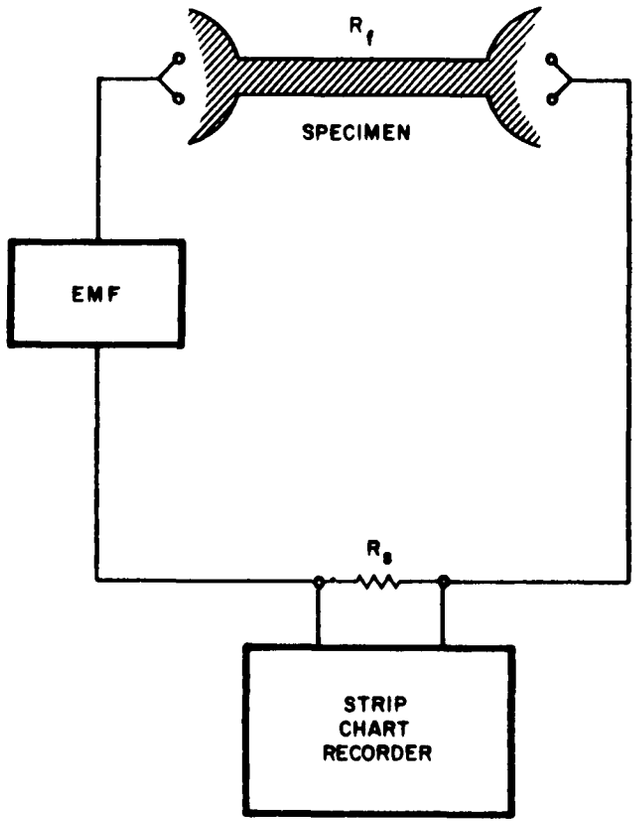

Figure 5 - Schematic of Circuit Utilized for Monitoring of Small Film Conductance. $\underline{R}_f$ Denotes the Film Resistance and $\underline{R}_s$ a Standard Resistance.

through pressed teflon seals at either end of the hollow rotatable shaft on which the mask holding wheel is mounted. With good thermal contact between quartz substrate and well, bringing the probes in contact with the substrate does not result in any measurable change in substrate temperature.

The circuit employed in conductance measurements is either that of Fig. 5 or that of Fig. 6. The former circuit was used for detection and recording of small conductances ($\sim 10^{-5}\ \Omega^{-1}$). The remainder of the deposition was monitored using the second circuit.

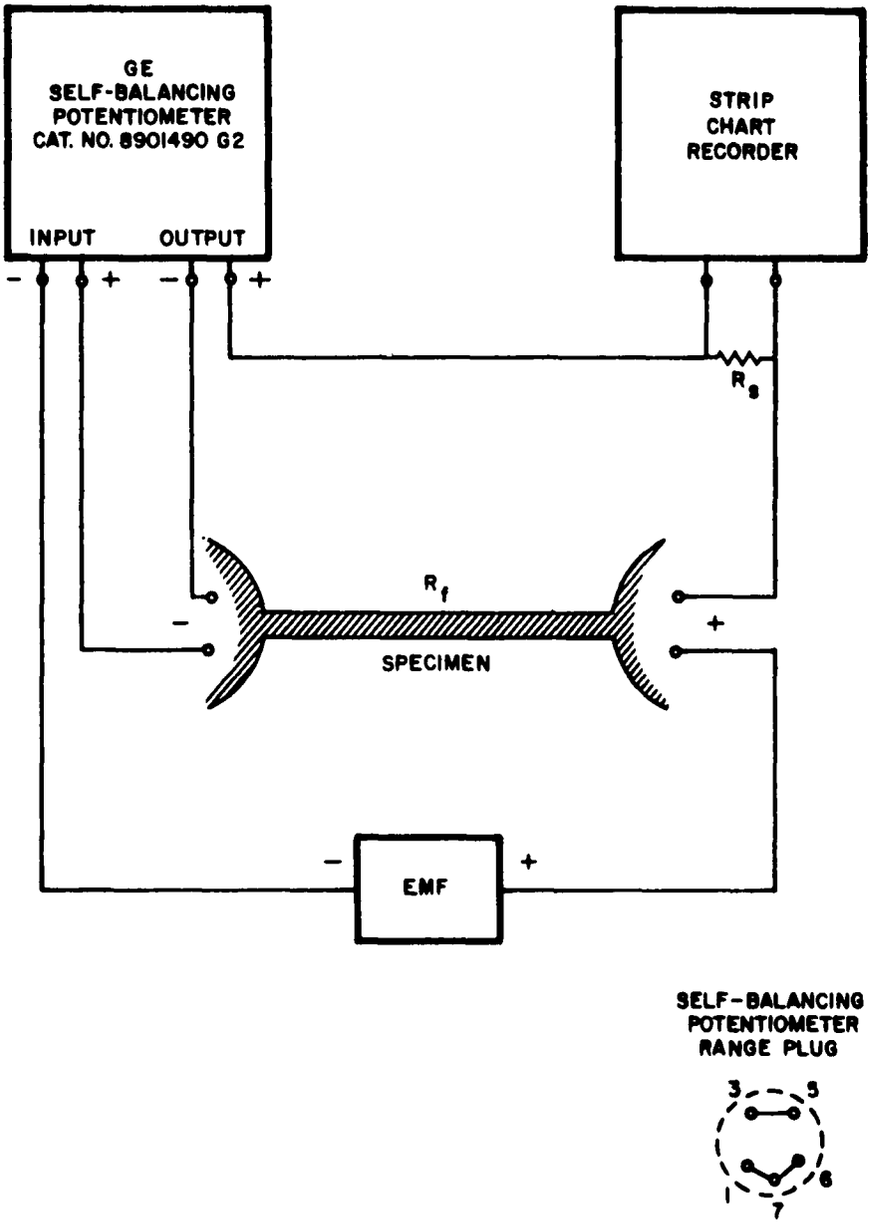

Figure 6 - Schematic Diagram of Film Conductance Monitoring Circuit Employing Self-Balancing Potentiometer. R_f denotes the Film Resistance and R_s a Standard Resistance.

This employs a self-balancing potentiometer to maintain a constant voltage across the film. The voltage driving the recorder will then always be strictly proportional to film conductance. This is true for the simpler circuit only if the standard resistance R_s is much less than the film resistance R_f. The current in the input loop of the self-balancing potentiometer is a microampere or less so that the effect of contact resistance should be negligible. This is important in ensuring that a given conductance, as indicated by a certain recorder deflection, corresponds to a given film conductance and hence thickness.

Provision was made for easy switching between circuits of different sensitivity so that the whole course of the deposition could be followed using two or three scales. A dual-channel Varian strip chart recorder having a chart speed of 8"/min. was used to record the conductances of two of the four films evaporated. A second was used to record pressure and monitor various temperatures, particularly substrate temperature, during deposition.

F. Film Thickness Measurements

The gate-film thicknesses were measured interferometrically either by the Tolansky method[6] or by a method which makes use of a modified Fabry-Perot interferometer.[7] The former method is accurate to about 200 Å, whereas the latter is accurate to about 25 Å. Film thicknesses were also calculated from values of room temperature resistance. Values of resistivity used in such calculations were 11.5×10^{-6} Ω-cm and 22×10^{-6} Ω-cm for tin and lead respectively. (Consistent with the results of Appendix A, no corrections were made for scattering of electrons at the walls of the film.) Taking into account measurement error, the thicknesses of lead film determined by these two methods agree. However, for tin films the thickness calculated from resistance was consistently about 20% lower than that measured interferometrically. Presumably this is accounted for by a somewhat higher film resistivity than pure bulk resistivity for this material.

G. Cryostat and Electrical Measuring Equipment

The cryostat used to obtain a low temperature environment is essentially that described in a previous report[8] and is shown along with the electrical measuring equipment in Fig. 7. A source of slowly rising current was provided by a sawtooth generator with adjustable sweep speeds. A sweep speed was selected which was sufficiently slow that use of slower sweep speeds traced out essentially the same curve. Curves were plotted directly on a Model 35 Moseley X - Y recorder. The lowest voltage sensitivity available, through use of a Model 425A Hewlett-Packard micro-volt ammeter as a preamplifier for the recorder, was 5μv/cm. Current sensitivity could be varied upward from 0.5 ma/cm. Current and voltage could be measured with about 1% accuracy using this arrangement.

Some difficulty was experienced with test specimen holders in obtaining good contact to the evaporated pads on the substrate. A spring loaded holder with lead-tipped contacts (Fig. 8) was designed and served well if the oxide was periodically removed from the lead contacts.

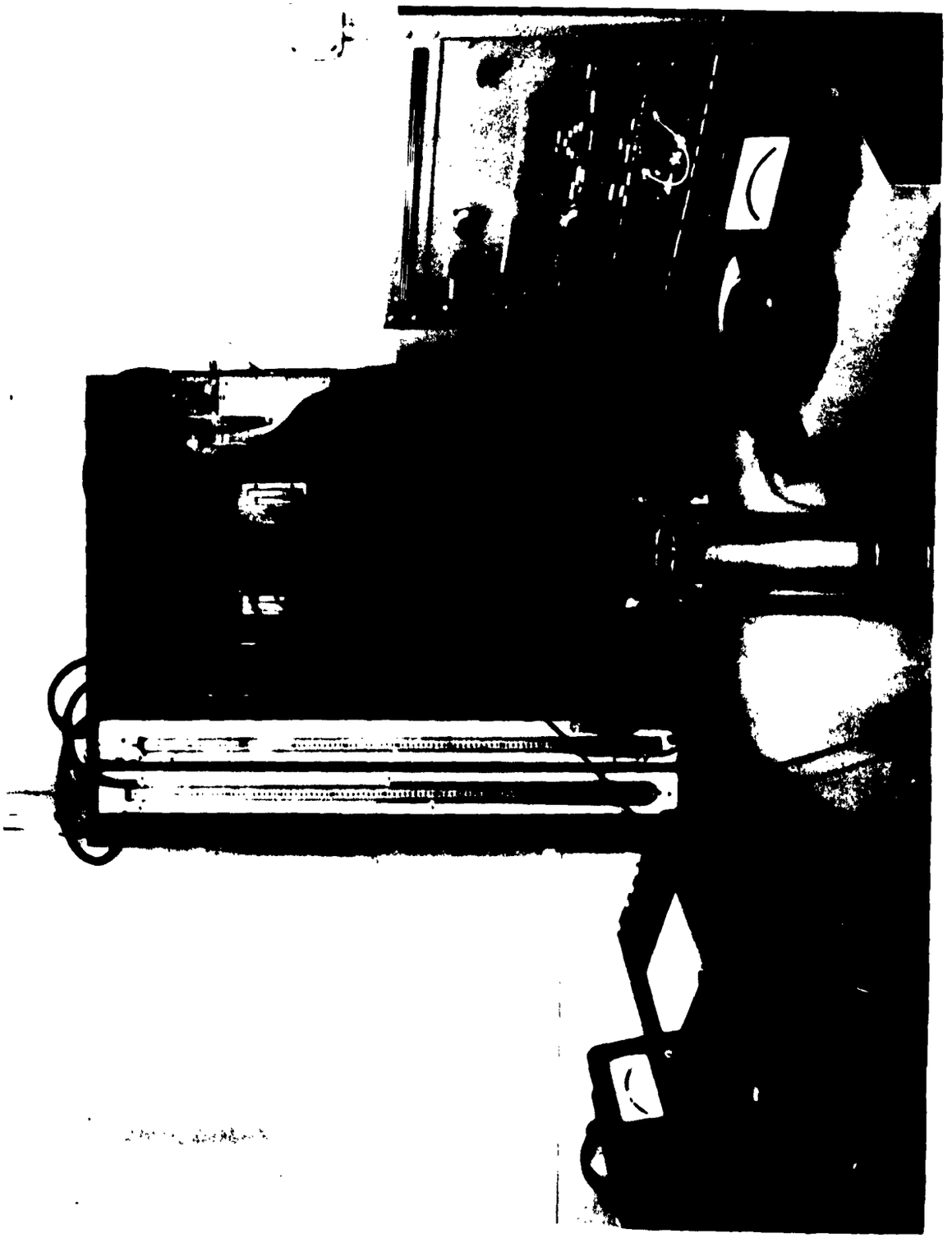

Figure 7 - Cryostat and Auxiliary Equipment Used in Low Temperature Measurements

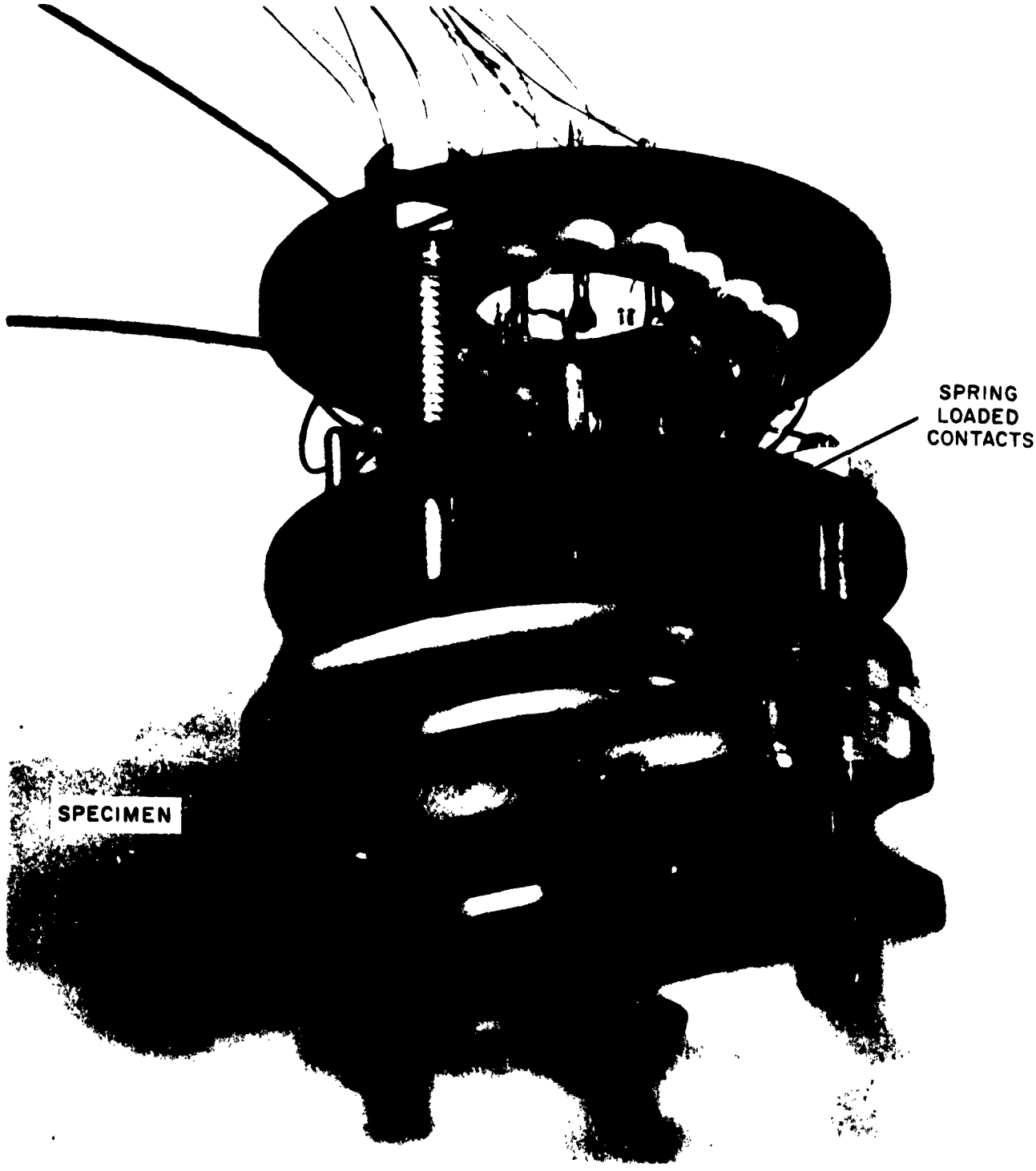

Figure 8 - Speciment Holder for Cryotron Test at Low Temperatures

III. DEPOSITION RESULTS

A. Control of Film Thickness

For the reproducibility measurements, deposition of tin and lead films was carried out at dry ice and acetone temperature (195° K). At this temperature and for a tin deposition rate of 27 Å/sec the conductance vs. time curve appears in Fig. 9. The exact form of the curve is quite dependent on deposition rate and substrate temperature. A detailed discussion of the conductance curves for tin and lead is given in Appendix A. The deposition was interrupted when the conductance reached a predetermined value. Two of the four specimens were monitored; in each case these two films reached the same conductance value in equal times (after correction for slight differences in film width). This indicates that effects of substrate roughness, stresses at film-substrate boundaries (and in the body of the film) and anisotropy are the same for all specimens, at least as regards their effect on electrical conductivity. Also they reached the same room temperature conductance so that the annealing properties are uniform from film to film.

The reproducibility in thickness realized using such a scheme is within a 5% range for different runs. Part of the variation is operator error since provision has not as yet been made for automatic closing of a shutter blocking the vapor stream as the conductance reaches a predetermined value. Also there is some difficulty in zeroing the recorder exactly due to drift in the instrument. The remainder of the fluctuation is probably due primarily to small variations in substrate temperature and deposition pressure or composition of residual gases, any of which might tend to change slightly the resistivity of the deposited material and hence the numerical relationship between conductance and thickness. No striking correlations of this nature have been noted however.

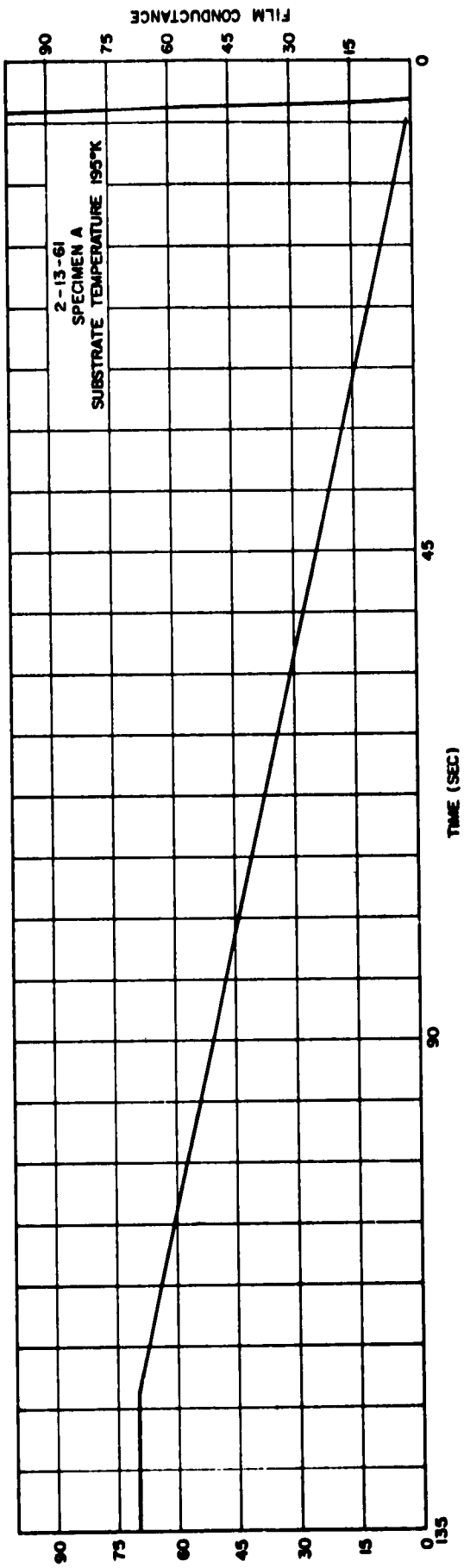

Figure 9 - Film Conductance as a Function of Time for Tin Deposited at a Rate ≈ 27 Å/sec. Conductance Units are Arbitrary.

B. Control of Film Edges

By using collimators to limit source size and positioning the mask within a mil of the substrate, lead films several microns thick have been formed with penumbra less than 1μ. An evaporated cross-film cryotron is shown in Fig. 10 along with a magnified view of the lead control film and a portion of the tin gate film. Note that the boundary of the tin film is also very distinct due to the agglomeration and separation of the edge when the tin film was heated to about 340°K. After several evaporations it was found that, for the lead films, scattering became more and more prevalent. This was due to build-up of lead on the front surface of the knife edges, thus allowing scattering of material in the shadows of the slits. Removal of previously deposited lead with a weak solution of acetic acid and hydrogen peroxide alleviated this situation.

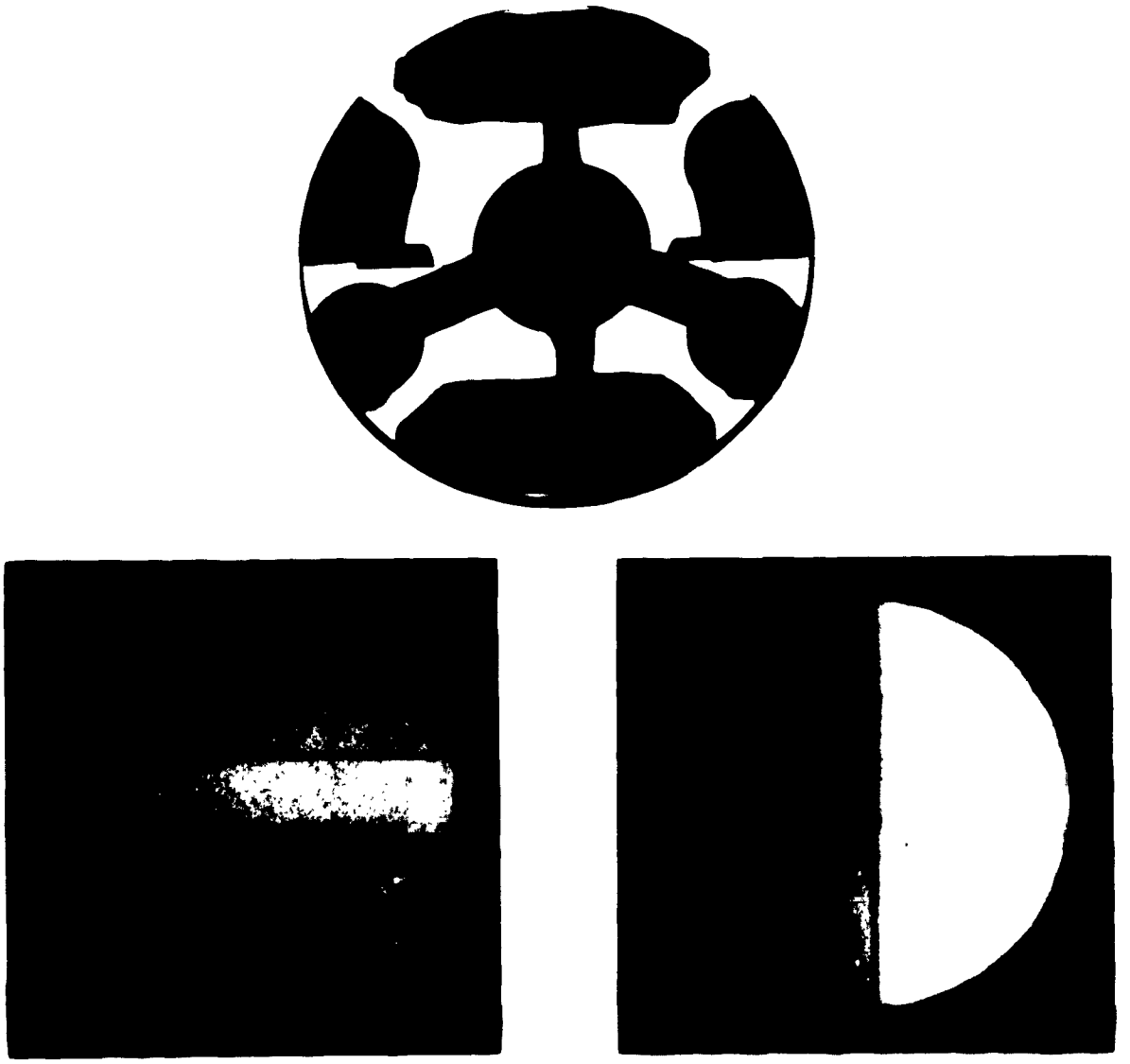

Figure 10 - Vacuum Deposited Thin-Film Cryotron With 480 Micron Gate and 23 Micron Control. The Lead Control Film on The Left and a Portion of the Tin Gate Film are Shown In the Bottom Photographs at 400 x Magnification. The Tin Film Proper is on the Extreme Right.

IV. ELECTRICAL AND SUPERCONDUCTIVE PROPERTIES OF FILMS

A. Low Temperature Resistance

The ratio of room temperature resistance to resistance at 4.2°K proved to be nearly constant at 50, there being only slightly more than ± 5% variation even with no account taken of the small range of gate thicknesses. The low temperature resistance can be fully accounted for in terms of random scattering of electrons at the walls of the film as given by the Sondheimer theory.[9] For low temperatures and moderately thin films ($l_o \gtrsim 10t$) the resistance is given by the approximate expression:

$$R(T) = \frac{l}{w}\,\rho_o(T)\,l_o(T)\,\frac{1}{t^2\,(0.34 + 1.7\log l_o/t)} \qquad (1)$$

where

l is the length of the film

w is the width of the film

t is the thickness of the film

$\rho_o(T)$ is the resistivity of bulk material of the same composition as the film (i.e., same number of lattice defects) at temperature T

$l_o(T)$ is the electron mean free path at temperature T for bulk material.

Taking $\rho_o\,(4.2^\circ K) = 1.8 \times 10^{-8}\ \Omega$-cm and $l_o\,(4.2^\circ K) = 15.8\mu$ leads to calculated resistances agreeing with the resistances measured for tin. These values of ρ_o and l_o were determined experimentally by measuring $R\ (4.2^\circ)$ for films of widely varying thickness. The largest film thickness employed was, however, still small compared with $l_o\ (4.2^\circ)$ so that Eq. 1 is valid. The slope of a log R, log t plot is then given simply by

$$\frac{d(\log R)}{d(\log t)} = -2 + \frac{1.7}{0.34 + 1.7\log l_o/t} \qquad (2)$$

and involves only the mean free path. Setting this expression equal to the slope of the experimental curve at a given thickness then determines l_o and from the magnitude of $\underline{R}$ (4.2) at that thickness, $\underline{\rho_o}$ (4.2) is determined.

Our value $\rho_o l_o = 2.8 \times 10^{-11} \Omega\text{-cm}^2$ compares favorably with values of $\rho_o l_o = 2.0 \times 10^{-11} \Omega\text{-cm}^2$ and $2.3 \times 10^{-11} \Omega\text{-cm}^2$ from measurements at 4^oK on thin tin foils [10] or along the c axis of a single crystal of tin [11] respectively.

B. Critical Temperature

A typical plot of gate voltage vs. gate current with control current as parameter is shown in Fig. 11. Critical temperatures for the gate film were determined to within 0.005^oK by varying the temperature of the helium bath in small steps and noting the first appearance of zero slope on such a plot. Although the critical temperatures were approximately 0.1^oK higher than that for bulk tin, nevertheless they were very reproducible, differing by no more than 0.005^oK.

C. Critical Currents

Currents of critical import are the gate current required (with no control current) for first appearance of gate resistance $\underline{I_t}$ and for restoration of the major portion of the gate resistance $\underline{I_c}$; also the control current $\underline{I_k}$, which makes resistive the entire portion of the gate directly under the control for gate currents approaching zero, and the gate current $\underline{I_\theta}$ which for this value of control current causes the entire gate to become resistive. These are indicated in Fig. 11.

Measurements of critical currents were made at several temperatures within about 0.6^oK of the critical temperature. The results for a number of cryotrons at three temperatures are included in Table I. All currents except $\underline{I_c}$ show variations of no more than $\pm 5\%$ for each of the three bath temperatures listed. The general dependence of these "critical" currents on bath temperature is shown in Fig. 12. This has been discussed in some detail elsewhere [12] along with the

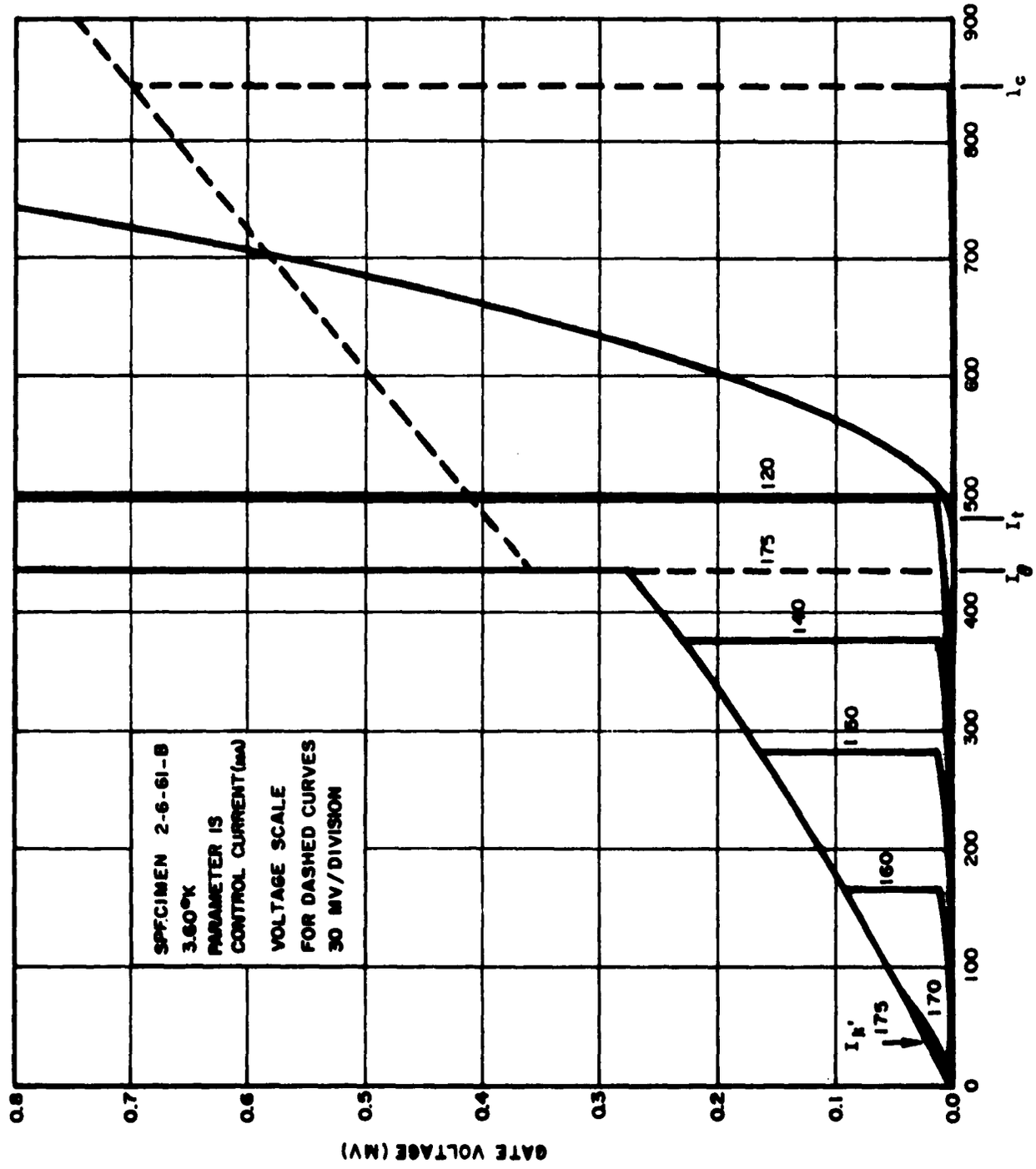

Figure 11 - Gate Voltage as a Function of Gate Current with Control Current as Parameter

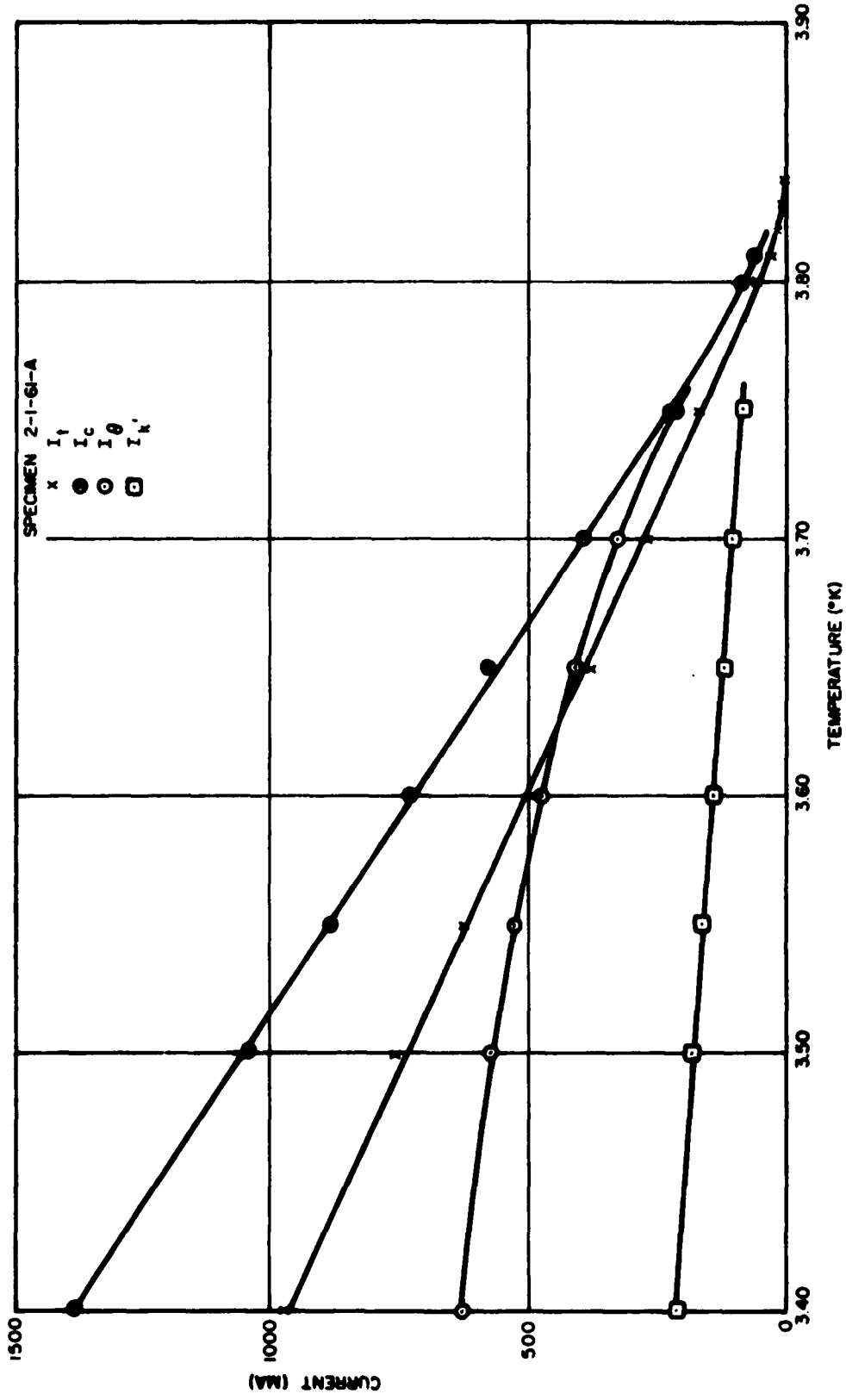

Figure 12 - Critical Currents for a Cryotron as a Function of Bath Temperature

importance of these currents in connection with operation of circuits employing cryotrons. It would be expected that I_c would show the greatest variation since it, being explained largely in terms of joule heating, is quite sensitive to the number of resistive sections of a bar; i.e., to the degree of imperfection in width or thickness of a film.

It is of interest that the variation quoted is the same whether we consider specimens made during a single evaporation or on subsequent evaporations. This indicates that such variations are of a random structural nature rather than characteristic of a particular set of evaporation conditions. Also, it is worthy of special note that the tin deposition rates were inadvertently varied by a factor of about three and this again led to no greater fluctuation in superconducting properties.

The initial slope of the gate voltage vs. gate current curve with I_k, flowing through the control is just the gate resistance lying under the control. Comparison of this resistance with the full gate resistance gives a measure of control width. It is found, within experimental error to be exactly what is measured optically so that, electrically speaking, the control edges are sharp to within the tolerance mentioned previously, of about one micron.

It should be mentioned that all measurements were carried out on cryotrons having a ground shield. Without a ground shield, transitions are not nearly as sharp and critical currents are lower. Ground shields also greatly reduce the self inductance of strips placed near them so that any application of cryotrons would almost surely employ ground planes.

V. ACKNOWLEDGEMENTS

The authors gratefully acknowledge the contributions of Dr. Fred W. Schmidlin in the planning and development of much of the apparatus and technique described. They are also indebted to Dr. John L. Rogers for valuable discussion during preparation of the report and E. R. Hartsfield for aid in the fabrication of test specimens.

APPENDIX A

BEHAVIOR OF FILM CONDUCTANCE DURING DEPOSITION

As films of lead and tin are deposited, the conductance vs. time curves can be observed for all ranges of conductance. Such measurements have been made for lead films deposited on substrates of widely varying temperature (300°K, 255°K, 195°K, 77°K) and for tin films (300°K, 195°K). At 195°K for both materials, the deposition rates were varied from a few Angstroms per second to about a hundred Angstroms per second. As might be anticipated, all curves have in common a region where no conductance occurs since initially the film is a series of islands of material which do not form an electrically continuous path. However, after conduction begins, the conductance has quite a varied behavior depending on substrate temperature and deposition rate. Fig. 13 shows a series of conductance curves for lead films formed at three different temperatures for a deposition rate of about 17 Å/sec. The conductances have been normalized so that the slopes of all curves, in the thicker film region, equal the slope of Curve 2. Presumably at some temperature between 77°K and 195°K a curve occurs which is essentially a straight line through the point where conduction is first recorded. This will be referred to as Curve 3. A near example of such a curve is that of Fig. 9.

The main features of the conductance curves may be explained in terms of scattering of conduction electrons at the walls of the film and migration of atoms (or small groups of atoms) along the surface of the substrate. Once this has been established, useful and interesting information can be extracted from the conductance curves regarding these two phenomena. The discussion will be divided into two sections. The first illustrates the manner in which interaction of the phenomena of wall scattering and that of surface migration determines specific forms for the conductance curves. Conclusions are then drawn regarding the exact nature of the wall scattering under varying conditions, i.e., whether random or spectral. The second section examines the changes in the

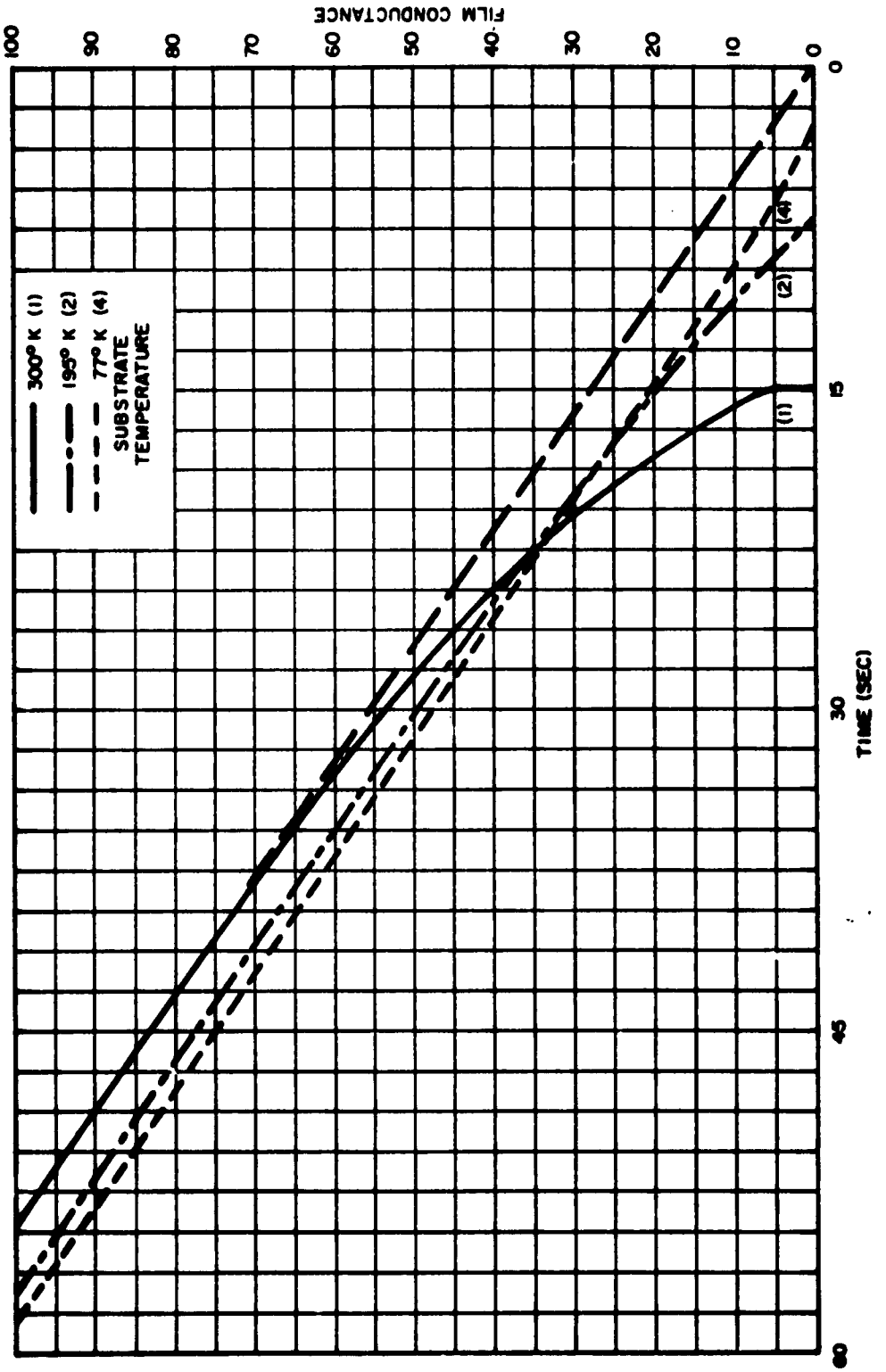

Figure 13 - Film Conductance as a Function of Time for Lead Deposited At Approximately 17 Å/sec on Substrates At Different Temperatures. Conductance Units Are Arbitrary.

delay time for conduction to begin with substrate temperature and deposition rate. What seems to be a minimum critical thickness for the onset of conduction in a given material is determined. This occurs for very large deposition rates, fairly independent of substrate temperature.

1. Shape of Conductance Curves

If a deposition is interrupted shortly after conduction begins, the conductance decreases if the substrate is maintained at that temperature. This is presumably because surface migration of atoms takes place and causes bunching in the film. Initially a large number of nuclei may be considered present, but some may grow at the expense of others. The phenomenon of surface migration is instrumental in both determining the delay times before electrical continuity is achieved and in shaping the initial portions of the conductance curve. As can be noted from Fig. 13, increasing substrate temperature, for a fixed deposition rate, involves a transition from curves (4) to (3) to (2) to (1). At a particular substrate temperature below room temperature, say 195°K, the sequence of curves having shapes (2), (3), (4) is passed through as the deposition rate increases. For low deposition rates, time is allowed for a significant amount of surface migration. If the substrate temperature is high, the surface mobility of the atoms is increased. Under either of these conditions a rougher film is formed initially and there is an appreciable time interval (convex portion of 2) where all parts of the film are being joined together. This time interval is even larger at 300°K, but quite small under conditions where Curve 3 or Curve 4 occurs. A conductance curve having convex shape, when viewed from the origin of coordinates, indicates that as the deposition proceeds, the rate at which isolated lands of material join the continuous portion of the film becomes smaller.

It seems reasonable that this would be true regardless of deposition rate or temperature of substrate. However, Curves 3 and 4 seem to represent a variation from this behavior. Another factor, the surface scattering mentioned on Page 23 must be considered. It is easily seen from Eq. 1 that such scattering leads to a conductance curve

which is concave toward the origin for small thicknesses, as observed in Curve 4 and effectively counter-balanced in Curve 3. Under conditions where Curves 1 or 2 are formed, Eq. 1 is probably not valid since at the time conduction begins, the islands of material have thicknesses which are several hundred angstroms and are therefore comparable with the electron mean free path.

For thicknesses much larger than the electron mean free path, film conductance $\underline{C}(T)$ at temperature $\underline{T}$, including effects of wall scattering, is given by the approximate expression:

$$C(T) = \frac{w}{l} \frac{t}{\rho_o(T)} \left[1 - \frac{3}{8} (1 - p) \frac{\ell_o(T)}{t} \right] \qquad (A.1)$$

where the symbols are those defined in Sec. IV with the exception of $\underline{p}$ which has values between zero and one corresponding respectively to purely random scattering or purely spectral scattering of electrons at the walls of the film. All conductance curves seem to behave in accordance with this relation at large thicknesses.

Referring to Fig. 13, it is noted that the linear portion of Curve 1 extrapolates back through the origin, within experimental error. This implies for deposition of lead at this temperature, at least for thicker films, that $p = 1$ so that wall scattering is purely spectral. The same conclusion is reached for tin deposited at room temperature since the conductance curve in this instance again has the form of Curve 1. For curves (2), (3), or (4), $\underline{p}$ is certainly less than one. We can obtain an exact value for $\underline{p}$ from Eq. A.1, provided $\underline{\ell_o}(T)$ is known, by simply extrapolating the linear portions of any one curve back to the time (or equivalently the thickness) axis and noting the value of the intercept. We have previously found $\underline{\rho_o \ell_o}$ at 4.2°K for tin. If it is assumed this product remains constant with temperature:

$$\rho_o(T_1)\, \ell_o(T_1) = \rho_o(T_2)\, \ell_o(T_2) \qquad (A.2)$$

Taking as value for ρ_o at 195°K the bulk value, then ℓ_o at 195°K can be calculated. Referring to Fig. 9 we find in this way that at 195°K for tin, p is about four-tenths. Lack of direct experimental knowledge concerning ℓ_o for lead prohibits calculation of p at reduced substrate temperatures.

If a deposition at a reduced temperature is interrupted when the film thickness lies in the linear region of the conductance curve and the substrate is allowed to reside at this temperature for a long period of time, no significant change in conductance occurs. If, however, the film is warmed to 300°K and recooled to the deposition temperature, one finds the conductance has risen to a point which lies on Curve 1. Annealing the films thus has the effect of making the wall scattering more spectral, i.e., the film surface smoother. Similar results in the annealing of gold films [13] have been observed. Here also p becomes larger as annealing is carried out. Such annealing can remove dislocations or, by expulsion of gas, cause closer packing of atoms and less resultant surface area.

All measurements in the reproducibility studies were made on tin films annealed at room temperature or above and as we have seen, such annealed films seem to exhibit purely spectral scattering. It is thus somewhat surprising that Eq. 1, which is valid for purely random scattering, fits the experimental resistances at 4.2°K. Possibly there is a change from spectral to random scattering as the ratio of film thickness to mean free path becomes smaller. What may be happening, in effect, is that in each process involving scattering of an electron at the surface of the film, some part of the knowledge concerning the initial direction of motion of the electron is lost. After many such processes the scattering could become randomized. However, this would be possible only if the electron experienced many encounters with the surface of the film between scatterings by a phonon or lattice imperfection, i.e., if the mean free path is large compared with film thickness. This sort of dependence of the nature of the scattering on l_o/t has been observed previously in cesium films [14] deposited at 70°K and in sodium wires [15] at 4.2°K.

2. Delay Time Before Onset of Electrical Conduction

The delay time before electrical continuity appears, when plotted against the reciprocal of the deposition rate, is shown in Fig. 14 for tin and in Fig. 15 for lead at three different substrate temperatures. For each point on these curves there is a critical thickness t_c, given by the product of deposition rate and delay time at that point, which must be deposited before conduction begins. The variation of critical thickness with reciprocal deposition rate appears in Fig. 16 for tin and in Fig. 17 for lead. Referring to the latter figure, we see that the critical thickness increases with decreasing deposition rate. This presumably results from the formation of larger, more widely-spaced islands of material due to the time allowed for surface migration of atoms at lower deposition rates. The increase in critical thickness with decreasing deposition rate for tin does not seem as pronounced as for lead. This is perhaps not unexpected since surface migration is felt to be more serious for lead than for tin.

If surface migration was the sole factor determining critical thickness then for very large deposition rates, the critical thickness should approach zero. This is not the case for either lead or tin. A possible reason for this is the statistical fluctuation in the uniformity of the vapor flux. It will surely not be continuous down to atomic dimensions, due to the discrete nature of the atoms, even if there is a very large number of atoms in the vapor stream. On this basis, the critical thickness extrapolated to infinitely large deposition rate should be independent of substrate temperature. Within the limits of experimental error indicated in Fig. 17, this seems to be the case. The error arises mainly from an uncertainty in the exact values of delay time. The uncertainty is a fixed amount regardless of deposition rate. Thus at high deposition rates, where the delay times are small, the uncertainty in delay time can be an appreciable part of the total value. Minimum values of critical thickness, given by the intercept on the critical thickness axis, appear to be in the range 80 Å to 90 Å for both lead and tin.

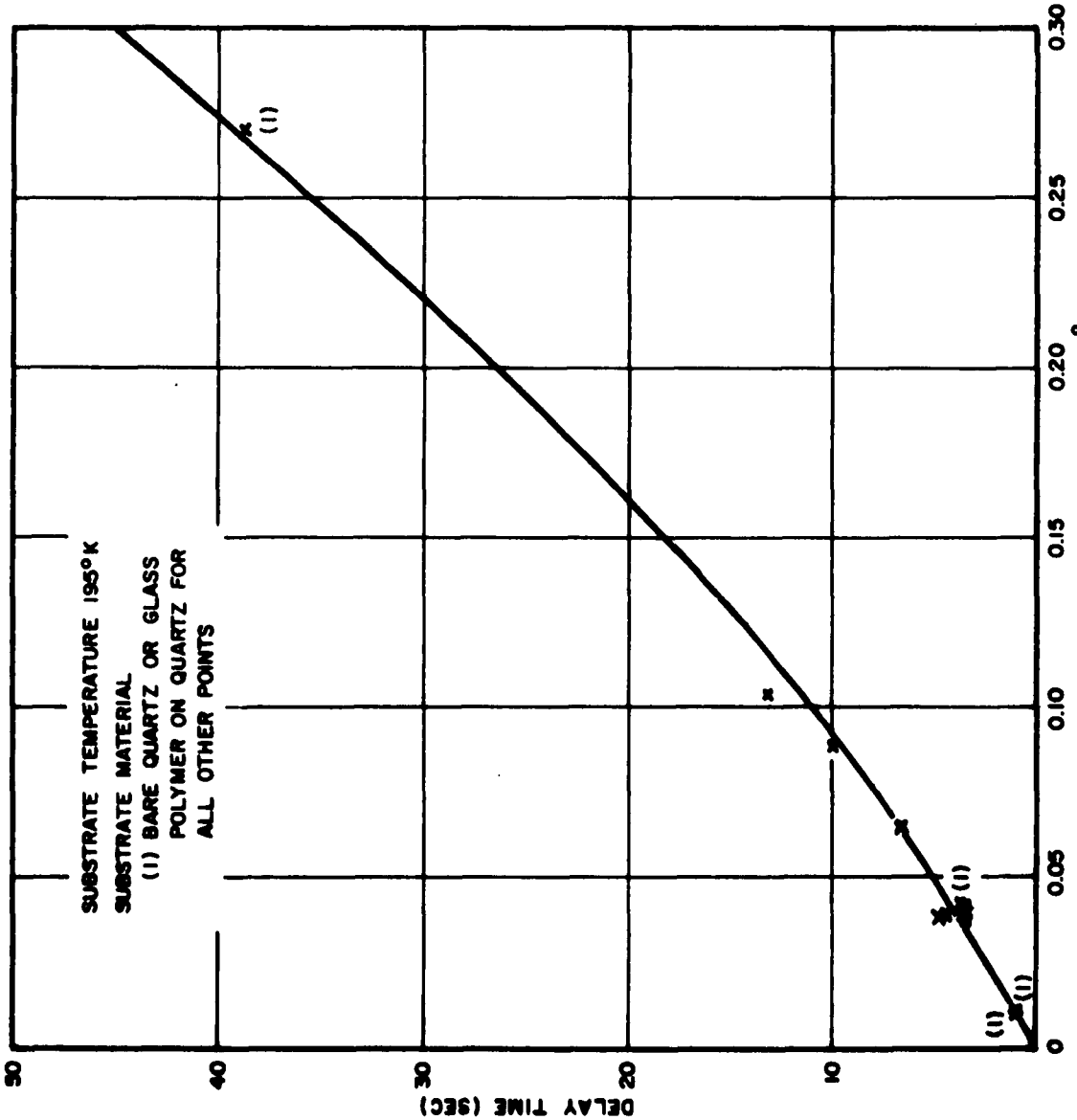

Figure 14 - Delay Time Before Achievement of Electrical Continuity As A Function of Reciprocal Deposition Rate For Tin Films

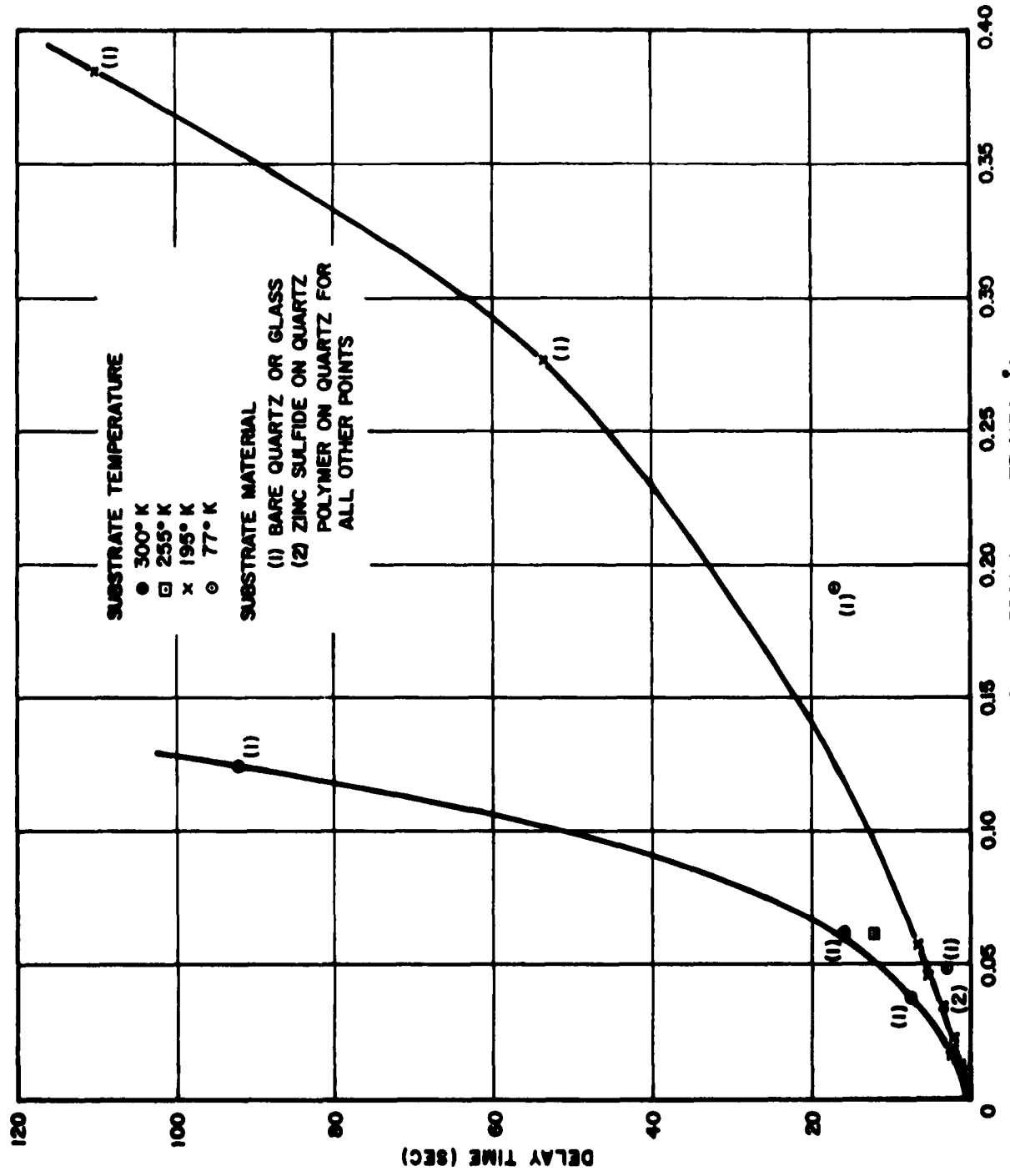

Figure 15 - Delay Time Before Achievement of Electrical Continuity As A Function of Reciprocal Deposition Rate For Lead Films

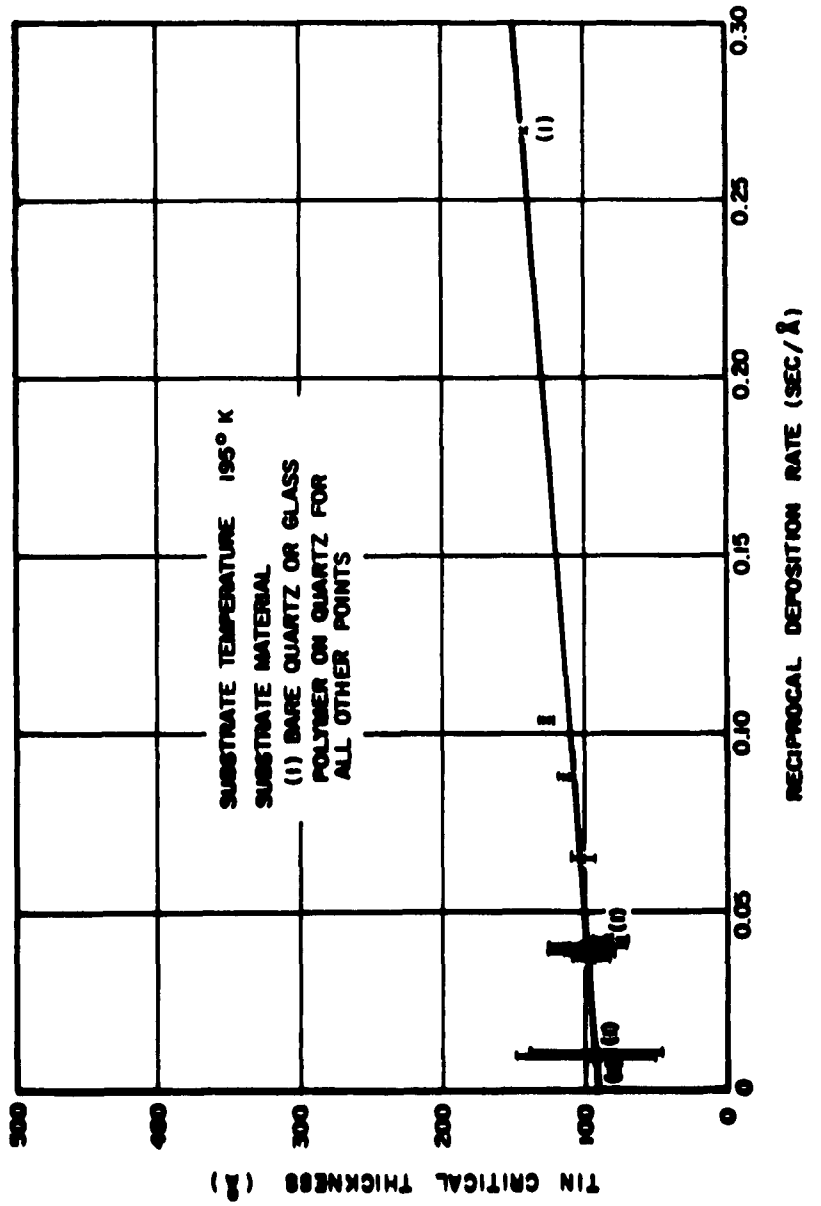

Figure 16 - Critical Thickness As A Function of Reciprocal Deposition Rate For Tin Films. Errors Indicated Arise From Uncertainty in Values of Delay Time.

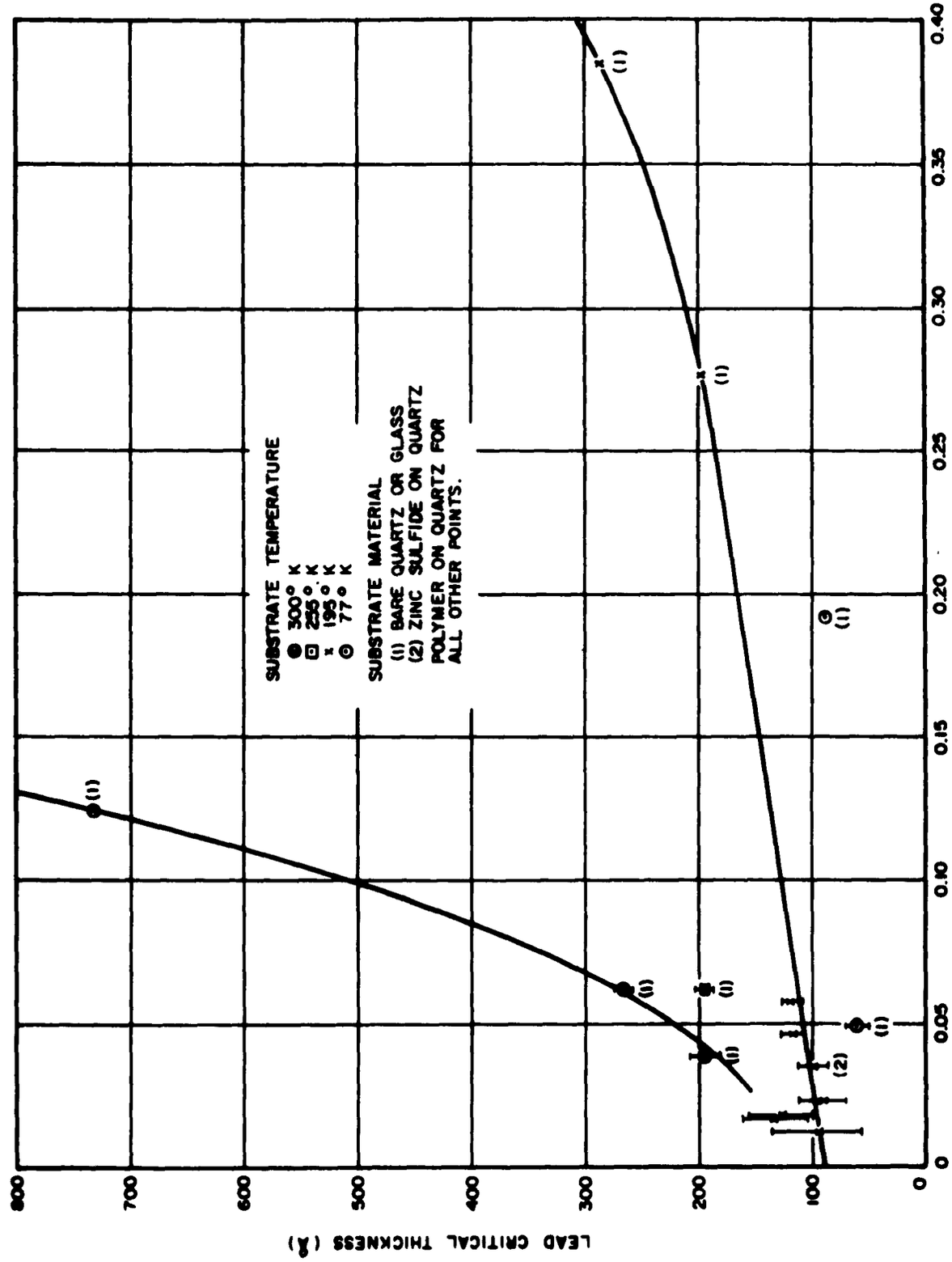

Figure 17 - Critical Thickness as a Function of Reciprocal Deposition Rate for Lead Films. Errors Indicated Arise From Uncertainty in Values of Delay Time.

Figure 18 shows the variation of critical thickness of lead films with substrate temperature for a moderate deposition rate of about 16 Å/sec. For this rate it appears that little is gained, in the way of more dense nucleation, by going from 195°K to 77°K. This is even more true for higher deposition rates where critical thicknesses, for all substrate temperatures, tend to the same value. The curve becomes nearly a horizontal line in this case. For smaller deposition rates perhaps the variation in critical thickness with substrate temperature is more exponential, rather than linear, at the higher temperatures.

Disregarding the actual distribution in size and shape of nuclei, we can get some idea of their average size at the time conduction begins by considering them to be uniform in size and hemispherical in shape. The relation between their diameter $\underline{D}$ and the critical thickness $\underline{t}_c$ is then given by $D = \frac{12}{\pi} t_c$. Thus, e.g., for the minimum critical thicknesses found above the average diameter of nuclei on this basis is somewhaht larger than 300 Å for both lead and tin.

For sufficiently low deposition rates it would be expected that a continuous film would not be formed, since the condensed atoms would be re-evaporated before an embryo nucleus could be formed. A relationship for the critical atomic beam density $\underline{n}_c$ has been given [16] as

$$n_c = C\, e^{-U/kT} \qquad \text{(A.3)}$$

where

C is a constant insensitive to temperature

U is the binding energy of condensed atoms to the substrate

T is the substrate temperature.

For silver on glass [17] at 465°K, $n_c \sim 3 \times 10^{10}$ atoms/cm^2/sec. We are working at much lower temperatures so $\underline{n}_c$ is presumably less than 10^{10} atoms/cm^2/sec. Our lowest deposition rates were still tremendously higher ($\sim 10^{15}$ atoms/cm^2/sec). It is also true that if atoms join

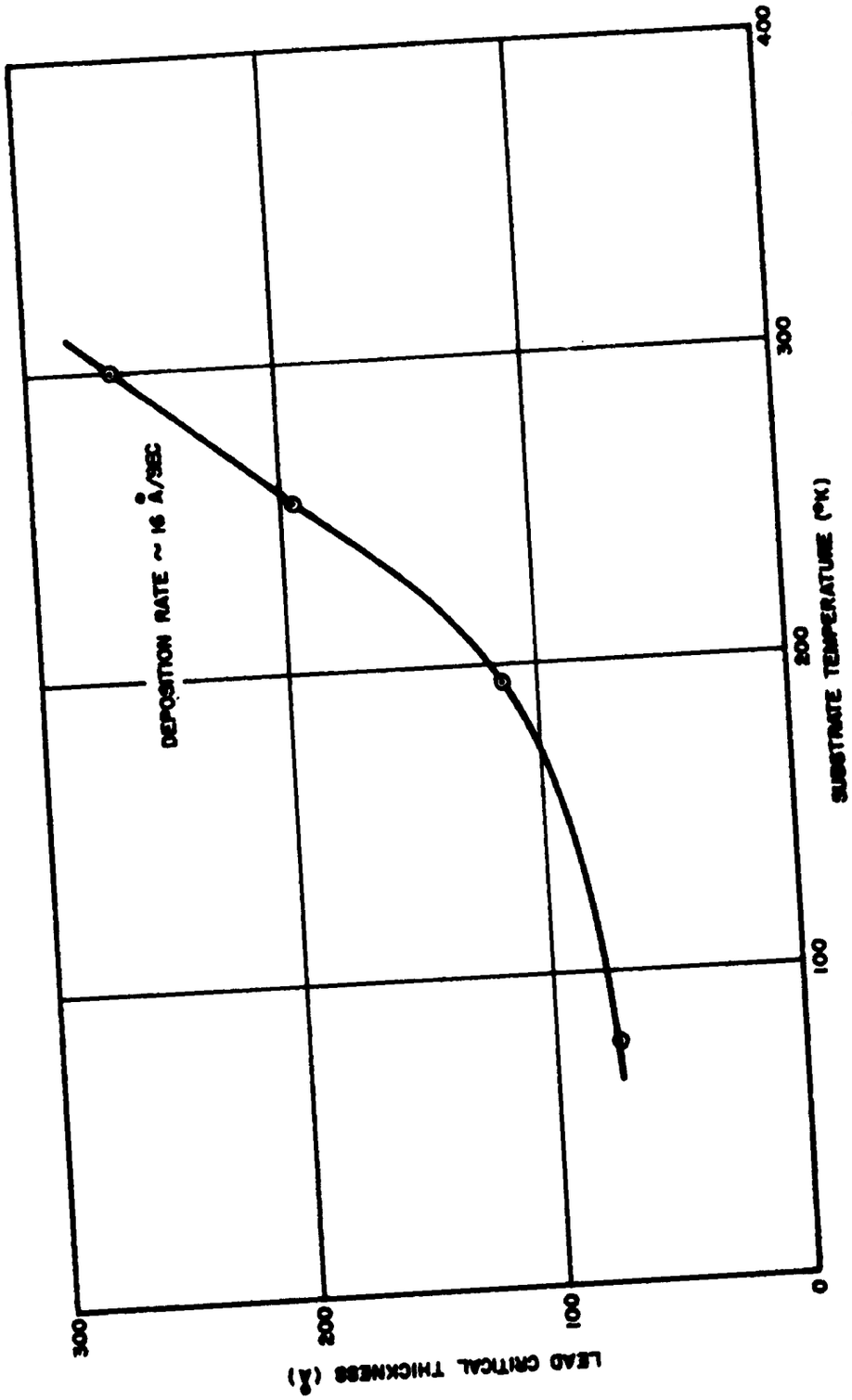

Figure 18 - Critical Thickness as a Function of Substrate Temperature for Lead Films

up in pairs they have even greater lifetimes before re-evaporation. Thus this phenomena could not have played a role in our measurements. The absence of re-evaporation does not rule out migration, however, since in general the activation energies for migration processes are quite low compared with those for evaporation.

It should be pointed out that the form of the conductance curves is not dependent on the particular variety of substrate material tested since behavior was identical with quartz, glass, mica, and zinc sulfide or polymer on quartz. It is however, possible that delay time results might have been quite different if deposition pressures were widely varied since absorbed gases on a substrate surface can have a profound effect on the mobility of condensed atoms.

APPENDIX B

TABLE OF CRYOTRON PROPERTIES

Glossary

Element Number	a specific letter A, B, C, or D refers to cryotrons formed from a particular set of one of the four sets of masks
Deposition Pressure	average pressure during period of evaporation onto substrate
Final Conductance	film conductance as indicated by strip chart recorder at cessation of evaporation onto substrate. Values in parenthesis are normalized to the width of A
Thickness, Interferometric	determined interferometrically by Tolansky method
	(a) determined interferometrically by modified Fabry-Perot method
Thickness, Resistance	calculated from film resistance measured at 300°K
Deposition Rate	calculated from interferometrically determined thickness
R(300°K)	total film resistance at room temperature
R(77°K)	total film resistance at liquid nitrogen temperature
R(4.2°K)	total film resistance at liquid helium temperature
R(3.7°K)	resistance of film excluding contact regions at 3.7°K
T_c	critical temperature
I_t	threshold current - gate current for first appearance of gate resistance
I_c	dc critical current - gate current for restoration of normal value of gate resistance

$I_{k'}$ critical control current - control current which for small gate current makes resistive the portion of the gate under the control

I_{θ} thermal propagation current - gate current which for the critical control current causes restoration of the entire value of gate resistance

Fixed Parameters of Cryotrons

Substrate	crystalline quartz
Deposition Temperature	195°K
Insulation Thickness (Nominal)	
Between Gate and Ground Plane	350 Å
Between Gate and Control	200 Å
Gate and Control Length	1.28 cm

Film Widths (in microns)

Element	A	B	C	D
Gate	480	480	470	460
Control (Average)	23.5	27.5	21.0	23.5
(At Gate)	23.0	26.5	19.0	23.0

TABLE I

Element Number		Deposition Pressure ($\frac{mm\ Hg}{\times 10^{-7}}$)	Final Conductance ($(ohm)^{-1}$)	Thickness Interferometric (Å)	Thickness Resistance (Å)	Deposition Rate (Å/sec)	Resistance R At 300°K (ohms)	Resistance R At 77°K (ohms)	Resistance R At 4.2°K (ohms)	Resistance R At 3.7°K (ohms)	R(300°K)/R(77°K)	R(300°K)/R(4.2°K)	T_c (°K)	I_t At 3.70°K (ma)	I_t At 3.60°K (ma)	I_t At 3.50°K (ma)	I_c At 3.70°K (ma)	I_c At 3.60°K (ma)	I_c At 3.50°K (ma)	I_{k^+} At 3.70°K (ma)	I_{k^+} At 3.60°K (ma)	I_{k^+} At 3.50°K (ma)	I_θ At 3.70°K (ma)	I_θ At 3.60°K (ma)	I_θ At 3.50°K (ma)	Ground Plane Thickness (Å)
2-1-61																										
GATE	A	6.5	0.125	3250(a)	2,620	9.6	11.7	2.42	0.232	0.228	4.83	50.3	3.84	270	500	760	395	735	1040	105	140	180	325	470	575	7,700
	B			3020	2,570	8.9	12.0	2.52	0.252	0.250	4.76	47.6	3.84	235	460	645	340	625	850	130	175	210	270	410	490	7,400
	C		0.122 (0.124)		2,600		12.1	2.54			4.77															
	D				2,550		12.6																			
CONTROL	A	4.3	0.0143	11,200	11,400	42.2	104.5	24.6			4.24															
	B			7,500	7,300	28.2	140	33.7			4.15															
	C		0.0124 (0.0140)	11,400	11,000	43.1	122	29.8			4.10															
	D				6,900		174	42.0			4.15															
2-6-61																										
GATE	A	4.7	0.125	3250(a)	2,570	15.3	12.0	2.49	0.232	0.230	4.82	51.7	3.84	260	500	765	460	875	1240	110	150	180	330	480	555	9,800
	B			3160	2,520	14.9	12.2	2.55	0.250	0.250	4.80	48.8	3.84	260	480	685	410	845	1230	130	175	215	300	435	520	11,000
	C		0.123 (0.125)		2,540		12.4	2.58			4.80															
	D				2,510		12.8	2.66			4.80															
CONTROL	A	3.3	0.0143	11,200	11,000	81.8	109	25.4			4.29															
	B			9,600	9,700	70.0	105.5	24.9			4.24															
	C		0.0130 (0.0147)	11,000	11,200	80.2	120	28.2			4.25															
	D				10,200		117	27.8			4.21															
2-13-61																										
GATE	A	4.8	0.125	3330(a)	2,590	27.1	11.9	2.47	0.243	0.240	4.81	49.0	3.835	270	510	775	495	925	1270	110	150	180	320	460	530	5,900
	B			3240(a)	2,590	26.3	11.9	2.51	0.250	0.249	4.75	47.7	3.84	275	505	755	465	825	1160	130	170	210	310	435	525	5,900
	C		0.123 (0.125)		2,580		12.2	2.54			4.80															
	D				2,590		12.4	2.59			4.79															
CONTROL	A	2.6	0.0143		11,000		109.5	25.8			4.25															
	B				11,500		88.5	20.9			4.23															
	C		0.0129 (0.0146)	11,300	11,100	57.7	121	28.3			4.27															
	D			11,800	12,100	60.2	99.5	23.3			4.27															
2-14-61																										
GATE	A	4.4	0.121*	3110	2,550	25.2	12.1	2.52	0.260	0.258	4.80	46.5	3.835	260	485	700	470	860	1210	110	145	180	300	435	500	14,000
	B			3030	2,500	24.5	12.3	2.56	0.260	0.260	4.79	47.3	3.84	250	480	685	420	725	1020	135	175	215	285	400	475	7,400
	C		0.119 (0.121)		2,540		12.4																			
CONTROL	A	2.8	0.0143	11,400	11,000	42.5	109	25.9			4.22															
	B				14,600		69.7	16.1			4.31															
	C		0.0132 (0.0149)																							

* Chart Paper Slipped

ADDITIONAL COMMENTS REGARDING ENTRIES IN TABLE I

It should first of all be noted that only the more complete families of elements on which low temperature measurements were made are listed in the table. Much preliminary work was carried out to establish the limits of reproducibility of gate thickness by monitoring resistance. Also additional evaporations were made to study in more detail the phenomena associated with the conductance curve.

The gate thickness for A specimens appears in general to be greater than that for B specimens. This may be due to a preferential tipping of the vapor source as it is brought into the jaws of the electrode prior to deposition. Misalignment of the lead vapor source and the collimators is most likely to occur along the circumference of the circle of rotation for the source. Misalignment in this dimension results primarily in an inequality of flux between the pairs A, C and B, D. This effect is readily evident for specimens 2-1-61.

The majority of measurements at liquid helium temperatures were made on specimens A and B since the gate width of these two cryotrons is exactly the same. This means I_t can be compared directly as measured for these cryotrons. On the other hand since the control widths were different, I_θ and $I_{k'}$ cannot be directly compared. Since $I_{k'}$ is directly proportional to control width, normalization to a common width can be carried out for this parameter. The exact variation of I_θ with control width is not known so comparison of I_θ must be made separately for A and B specimens. The data indicates an inverse dependence of I_θ on control width changing by a factor of 1.07 for control widths differing by a factor of 1.15. To take into account slight gate thickness variations, critical currents were plotted versus gate thickness, and a straight line drawn through the points. Variations of critical currents quoted are deviations from this line.

REFERENCES

1. Schmidlin, F. W., A. J. Learn, E. C. Crittenden, Jr., and J. N. Cooper, Solid State Electronics 1, 323-334 (1960)
2. Crittenden, E. C., Jr., J. N. Cooper, and F. W. Schmidlin, STL/TR-60-0000-NR356 (November 1960)
3. Crittenden, E. C., Jr., J. N. Cooper, F. W. Schmidlin, and A. J. Learn, "Structures and Properties of Thin Films" p. 282, Wiley, New York (1959)
4. Caswell, H. L., J. App. Phys. 32, 105 (1961)
5. Christy, R. W., J. App. Phys. 31, 1680 (1960)
6. Tolansky, S., "Multiple Beam Interferometry of Surfaces and Films" Oxford University Press, London (1949)
7. Schulz, L. G., J.O.S.A. 40, 690 (1950)
8. Crittenden, E. C., Jr., J. N. Cooper, and F. W. Schmidlin, Proc. I.R.E. 48, 1233 (1960)
9. Sondheimer, E. H., Advances in Physics 1, 1 (1952)
10. Andrew, E., Proc. Phys. Soc. A.62, 77 (1949)
11. Kunzler, J., and C. Renton, Phys. Rev. 108, 1397 (1957)
12. "Annual Report on Research on Low-Temperature Computing Elements" Space Technology Laboratories, Inc., STL/TR-60-0000-NR353, 30 September 1960
13. Gillham, E. J., J. S. Preston, and B. E. Williams, Phil. Mag. 46, 1051 (1955)
14. Appleyard, E. T. S., and A. C. B. Lovell, Proc. Roy. Soc. A.158, 718 (1937)
15. MacDonald, D. K. C., and K. Sarginson, Proc. Roy. Soc. A. 203, 223 (1950)
16. Frenkel, J., Z. Phys. 26, 117 (1924)
17. Yang, L., M. Simnad, and G. Pound, Acta. Metal. 2, 470 (1954)